Nuclear Physics B143 (1978) 189–231

PARTIAL-WAVE ANALYSIS OF $K^- p \to \pi^{\mp} \Sigma^{\pm}(1385)$ BETWEEN 1775–2170 MeV INCLUDING NEW DATA BELOW 1960 MeV

Rutherford Laboratory – Imperial College Collaboration

W. CAMERON, B. FRANEK, G.P GOPAL, G.E. KALMUS, A.C. McPHERSON and R T ROSS *
Rutherford Laboratory

T.C. BACON, I BUTTERWORTH, R W.M. HUGHES, P NEWHAM, R A. STERN and R.M. WATERS
Imperial College, London

Received 1 March 1978

New data are presented for the reaction $K^- p \to \Lambda \pi^+ \pi^-$ at 11 energies between 1775 and 1957 MeV in the centre-of-mass New values for the masses and widths of the $\Sigma^{\pm}(1385)$ are given The differential cross sections and the complete spin density matrices for the reactions $K^- p \to \pi^{\pm} \Sigma^{\mp}(1385)$ were extracted from these data using also the information from the Λ decay An energy-dependent partial-wave analysis has been carried out over the c m range 1775–2170 MeV also using data from an earlier experiment. Comparisons between the observed resonant amplitudes and SU(3) and $SU(6)_W \otimes O(3)$ predictions have been made

1. Introduction

The reaction

$$K^- p \to \Lambda \pi^+ \pi^- \quad \hookrightarrow p \pi^- \qquad (1)$$

has been investigated at 11 incident momenta between 0.96 and 1.355 GeV/c. The quasi two-body processes

$$K^- p \to \pi^- \Sigma^+(1385)\,, \qquad (2)$$

$$\pi^+ \Sigma^-(1385)\,, \qquad (3)$$

* Present address University of Michigan, Physics Department, Ann Arbor, Michigan 48109, USA

dominate reaction (1) and data for these channels have been extracted using a four variable fitting technique.

The new high-statistics data have then been combined with those of the CRSS Collaboration over the momentum range 1.263 to 1.843 GeV/c [1], and a partial-wave analysis has been carried out over the c.m. energy range 1775 to 2170 MeV.

2. Data

The new data for the reaction

$$\begin{aligned} &K^- p \to \Lambda \pi^+ \pi^- \\ &\qquad \hookrightarrow p \pi^- \end{aligned}$$

used in this analysis come from an exposure of the CERN 2m HBC to a K^- beam at 11 equally spaced incident momenta between 0.96 GeV/c and 1.355 GeV/c. Only events with two outgoing charged particles and seen neutral decay have been used. Details of the exposure, scanning and measuring, beam calibration and cross-section normalisation are given in an earlier publication [2].

Events with two-prong plus V^0 topology arise not only from reaction (1) but also from reactions

$$\begin{aligned} &K^- p \to \bar{K}^0 p \pi^- \\ &\qquad \hookrightarrow \pi^+ \pi^- , \end{aligned} \tag{4}$$

$$\begin{aligned} &K^- p \to \Sigma^0 \pi^+ \pi^- \\ &\qquad \hookrightarrow \Lambda \gamma \\ &\qquad\quad \hookrightarrow p \pi^- . \end{aligned} \tag{5}$$

Kinematical ambiguities between reactions (1) and (4) were resolved on the basis of ionisation measurements. Events which were kinematically ambiguous between reactions (1) and (5) proved overwhelmingly to be from reaction (1), as may be seen from the distribution of the missing mass to the $\pi\pi$ system (fig. 1). Also when ambiguous events from any missing mass region of fig. 1 are assigned to reaction (5) a marked anisotropy in the $\Sigma \to \Lambda\gamma$ decay angular distribution is observed. Accordingly, all ambiguous events have been assigned to reaction (1).

In order to correct for biases in the data, the following cuts and weights were applied.

(a) A cut of 0.3 cm ($l_{\min}$) was applied to the projected decay length of the Λ and the remaining events were each weighted by the inverse probability that the Λ would decay between $l_{\min}$ and the boundary of the fiducial volume.

$$P = \exp(-l_1/\bar{l}) - \exp(-l_2/\bar{l}) , \tag{6}$$

where $l_1 = l_{\min}/\cos\alpha$, α is the dip of the Λ, l_2 is the potential decay length from the

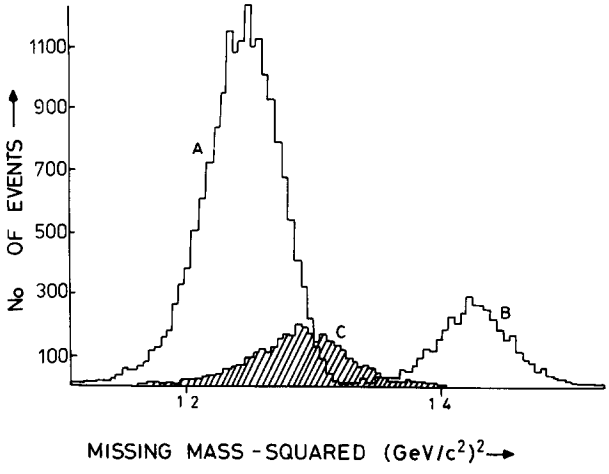

Fig 1 The missing mass-squared distribution to the $\pi^+\pi^-$ system for (A) unique $\Lambda^0\pi^+\pi^-$ events, (B) unique $\Sigma^0\pi^+\pi^-$ events, (C) events which are ambiguous between $\Lambda^0\pi^+\pi^-$ and $\Sigma^0\pi^+\pi^-$

production vertex to the boundary of the fiducial volume and $\bar{l} = pc\tau/M$ with $\tau(\Lambda) = 2.61 \times 10^{-10}$ s [3] and p and M are the momentum and mass of the Λ.

(b) Losses of Λ's due to slow particles from the Λ decay were corrected for by imposing minimum momentum cuts. These correspond to cuts in the cos δ distribution where δ is the angle between the decay track in the rest frame of the Λ and the Λ direction. A minimum momentum cut of 54 MeV/c was chosen for the pion but no cut was necessary for the proton A weight $W = 2/(1 - \cos\delta_1)$ was applied to the remaining events where δ_1 is the value of δ corresponding to a 54 MeV/c pion from the observed Λ.

The possibility of a loss of events with the decay plane perpendicular to the chamber window was investigated. No such loss was observed.

The final weight for each event includes scanning and throughput efficiencies. Numbers of events remaining after the cuts together with the average weight and the value of the cross section for reaction (1) at each of the incident momenta are given in table 1. The total number of events used was 23 885 The cross section as a function of momentum is shown in fig. 2 and is in good agreement with the results of earlier experiments [4–6].

Dalitz plots, together with their projections are shown in fig. 3 for the lowest, central and the highest incident momenta. The prominent features to be seen are two bands corresponding to the $\Sigma^-(1385)$ and the $\Sigma^+(1385)$ resonances. Some ρ production is also present at higher energies The $\Lambda\pi^+$ and $\Lambda\pi^-$ mass-squared distributions in the region of the $\Sigma^{\pm}(1385)$ ($1\,68 < M^2(\Lambda\pi) < 2.18$ (GeV/c^2)^2) obtained by summing data from all eleven momenta are shown in fig 4 The mass and width of each charge state of the resonance have been determined by fitting to each

Table 1
Values of cross sections for the $\Lambda^0 \pi^+ \pi^-$ final state and for processes contributing to it at the 11 incident beam momenta

Beam momentum (GeV/c)	c m. energy (MeV)	No of events after cuts	Average weight	$\sigma[K^- p \to \pi^- \Sigma^+(1385)]$ (mb)	$\sigma[K^- p \to \pi^+ \Sigma^-(1385)]$ (mb)	$\sigma[K^- p \to \Lambda \pi^+ \pi^-(\text{LIPS})]$ plus $\sigma[K^- p \to \rho \Lambda]$ * (mb)	$\sigma[K^- p \to \Lambda \pi^+ \pi^-]$ (mb)
0 960	1775	1508	1 26	1 26 ± 0 12	1 98 ± 0 17	0 85 ± 0 11	4 09 ± 0 17
1 005	1796	1350	1 25	1 12 ± 0 12	1 99 ± 0.19	0 94 ± 0 13	4 05 ± 0 18
1 045	1815	2235	1 26	1 29 ± 0 11	2 06 ± 0 15	1 16 ± 0 11	4 51 ± 0.16
1 085	1833	1970	1 24	0 97 ± 0 09	1 90 ± 0 15	1 06 ± 0 11	3 94 ± 0 15
1 125	1852	2058	1 22	0 98 ± 0 09	1 76 ± 0 13	0.92 ± 0 09	3 66 ± 0 13
1 165	1870	2214	1 22	0.95 ± 0 08	1 54 ± 0 11	0 68 ± 0.07	3 17 ± 0 11
1 205	1889	2182	1 22	0.88 ± 0 08	1 43 ± 0 11	0 73 ± 0 08	3 04 ± 0 11
1 245	1907	2593	1 21	0 90 ± 0.07	1 24 ± 0 09	0 67 ± 0 07	2.81 ± 0 09
1 285	1926	2668	1 21	0 84 ± 0.06	1.09 ± 0 07	0 71 ± 0.06	2 64 ± 0.08
1 320	1941	2195	1 23	0 82 ± 0.07	1 03 ± 0 08	0 76 ± 0 07	2 61 ± 0.09
1 355	1957	2912	1.20	0 74 ± 0 05	0 91 ± 0 06	0 70 ± 0 05	2 35 ± 0 07

* The cross sections determined for the LIPS and $\rho \Lambda^0$ have been added together as it was found difficult to separate them reliably.

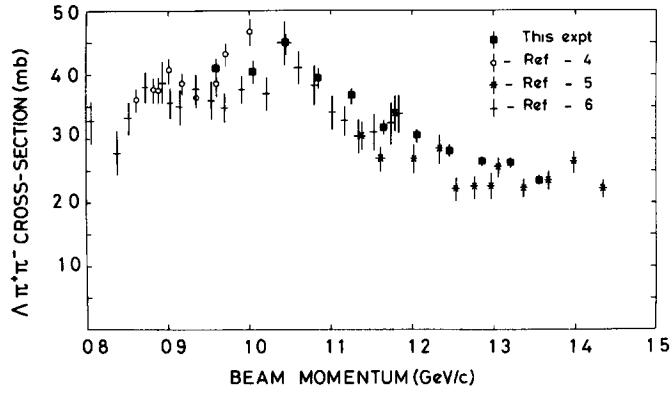

Fig 2 $K^-p \to \Lambda^0\pi^+\pi^-$ cross section as a function of incident momentum

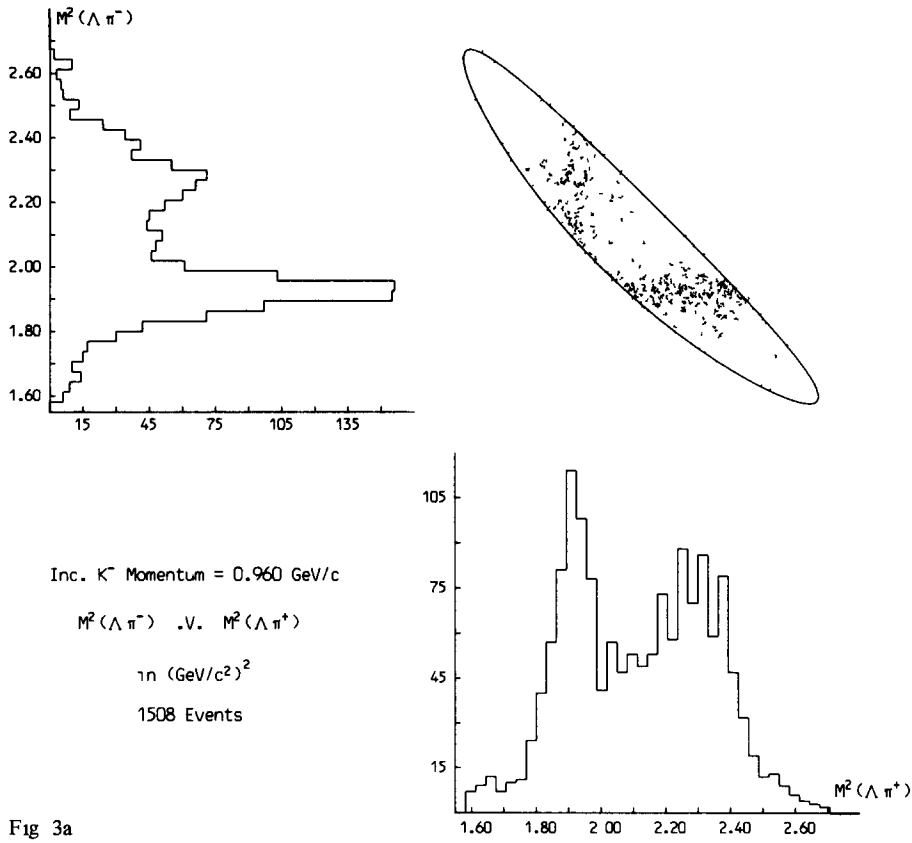

Fig 3a

distribution a relativistic Breit-Wigner shape superimposed on a linear background. Three different forms of the resonance shape have been tried· a relativistic Breit-Wigner [7] shape with energy independent width (FIT 1), the form used by Holmgren et al. [8] (FIT 2), and a P wave relativistic Breit-Wigner [7] (FIT 3) The results are given in table 2. The experimental resolution of approximately 2 MeV has been considered in the fits. In all three cases, higher order background forms have been tried but did not result in any significant improvement. However, they have an influence on the resonance parameters, especially the width and this uncertainty has been included in the quoted errors. As can be seen from table 2 and as confirmed by other experiments [8,9], good fits to the $\Lambda\pi^{\pm}$ spectra could not be obtained using a P wave Breit-Wigner form (FIT 3) A satisfactory description of the data is given by the other two forms of the resonance shape. However, we prefer the form with energy independent width since that gives the simplest description of the data. The values obtained are in excellent agreement with the average values pub-

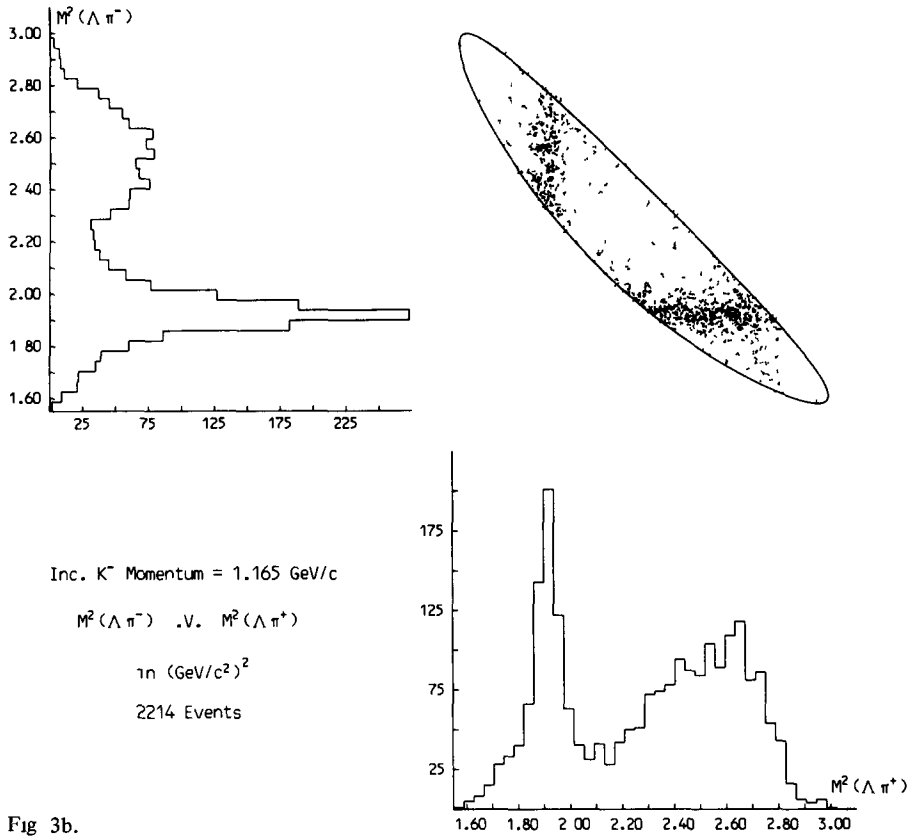

Fig 3b.

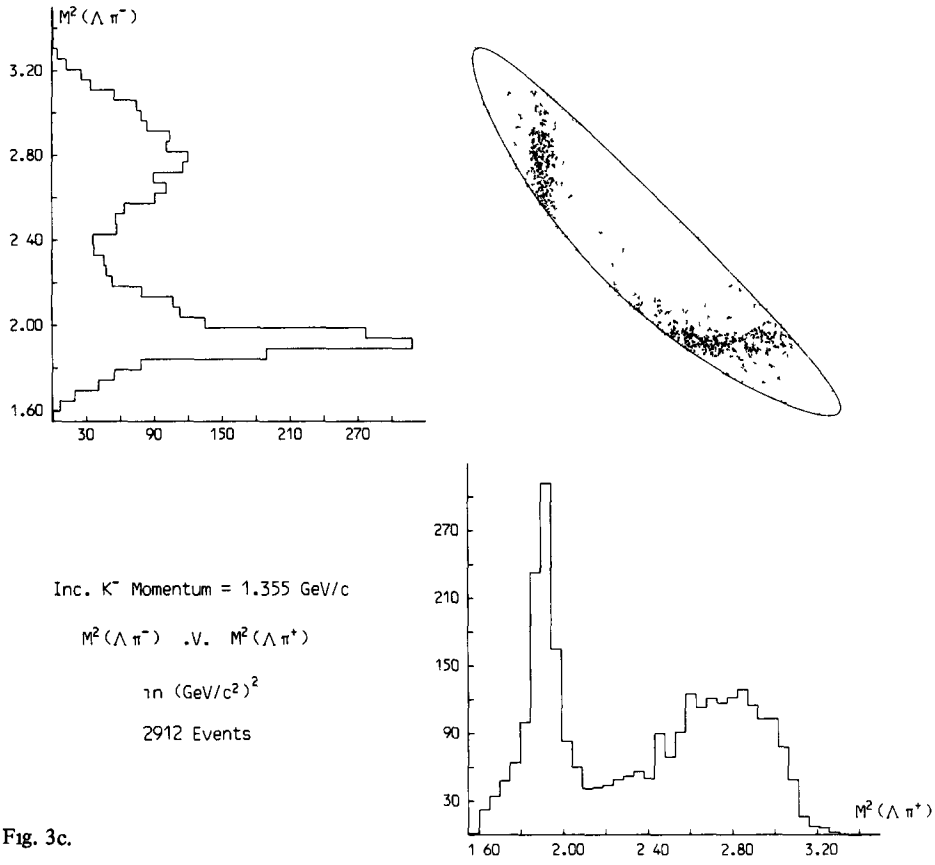

Fig. 3c.

Fig. 3 Dalitz plots of $M^2(\Lambda\pi^-)$ *versus* $M^2(\Lambda\pi^+)$ and projections at 0.960, 1 165 and 1.355 GeV/c K^- incident momenta for the reaction $K^-p \to \Lambda^0\pi^+\pi^-$

lished in the Particle Data Group tables [10] and represent by far the best determination of these parameters to date.

3. Extraction of the $\pi^{\mp}\Sigma^{\pm}(1385)$ channels

In order to extract $\pi^{\mp}\Sigma^{\pm}(1385)$ channels, reaction (1) has been considered as an incoherent sum of Lorenz invariant phase space and the three reactions:

$$K^-p \to \pi^-\Sigma^+(1385)\,, \tag{2}$$

$$K^-p \to \pi^+\Sigma^-(1385)\,, \tag{3}$$

$$K^-p \to \rho\Lambda\,. \tag{7}$$

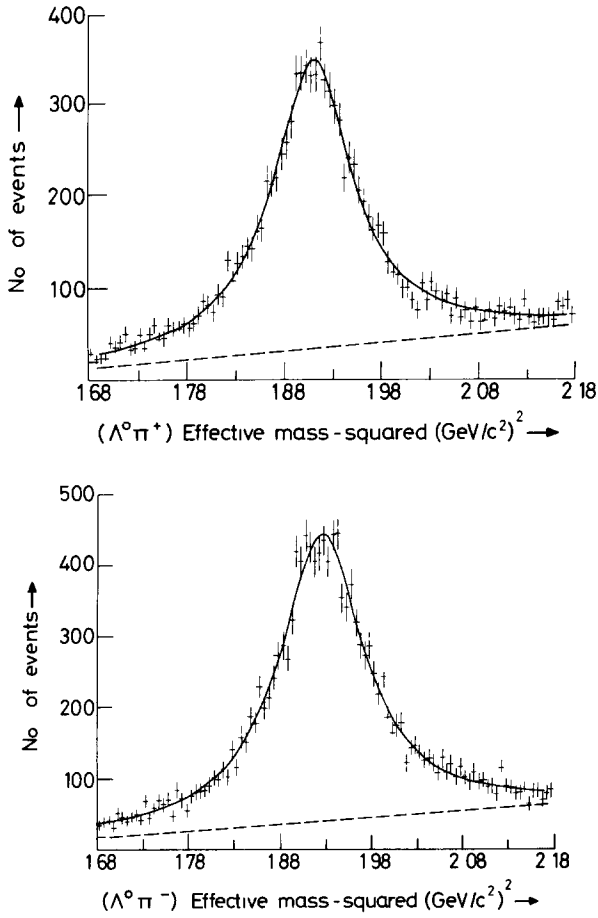

Fig. 4. (a) $\Lambda\pi^+$ and (b) $\Lambda\pi^-$ mass-squared distributions in the region of the $\Sigma(1385)$ resonance The curves are the result of the FIT 1 described in the text, the dashed line indicates the background under the resonance

The coefficients of the Legendre polynomial expansions of the differential cross sections and the real parts of the density matrix elements for the quasi two-body processes are extracted simultaneously [11]. The fact that the data are well fitted at all energies by an incoherent production model suggests that interference effects are small. A set of one-dimensional projections for a typical momentum (1.245 GeV/c) together with the results of the fit are shown in fig. 5 The probability distribution W for reactions (2) and (3) is given by

$$W(\cos\theta^*, \theta, \phi, M^2) = \frac{3}{4\pi} B(M^2) \frac{1}{\sigma} \frac{d\sigma}{d\cos\theta^*}$$

Table 2
Masses and widths of the $\Sigma^{\pm}(1385)$

		This experiment		χ^2/NDF	Number of events above background
		Mass (MeV/c^2)	Γ (MeV/c^2)		
FIT 1	Σ^+	1381 9 ± 0 3	35 5 ± 1 9	79 5/96	6900
	Σ^-	1387 6 ± 0 3	39 2 ± 1 7	111/96	9720
FIT 2	Σ^+	1383 5 ± 0 4	36 3 ± 1 9	102/96	6730
	Σ^-	1389 4 ± 0 4	41.1 ± 1 9	115/96	9640
FIT 3	Σ^+	1382 2 ± 0 4	37 5 ± 2 1	152/96	7000
	Σ^-	1388 3 ± 0 4	44 0 ± 2 0	155/96	10100
		Particle data table values			
		Mass (MeV/c^2)	Γ (MeV/c^2)		
	Σ^+	1382 5 ± 0 5	35 2 ± 1 7		
	Σ^-	1386 6 ± 1.2	42 4 ± 4 2		

$$\times \left[\tfrac{1}{2}(\tfrac{1}{3} + \cos^2\theta) + 2(\tfrac{1}{3} - \cos^2\theta)\,\rho_{33}(\cos\theta^*) - \frac{2}{\sqrt{3}}\sin 2\theta\cos\phi\,\mathrm{Re}\,\rho_{31}(\cos\theta^*) - \frac{2}{\sqrt{3}}\sin^2\theta\cos 2\phi\,\mathrm{Re}\,\rho_{3-1}(\cos\theta^*)\right], \tag{8}$$

where θ^* is the centre-of-mass scattering angle of the pion, θ, ϕ are the decay angles in the helicity frame of the $\Sigma(1385)$, M^2 is the invariant $(\Lambda\pi)$ mass squared and $B(M^2)$ is the relativistic Breit-Wigner form normalised to unity over the available phase space and with an energy-independent width for the $\Sigma(1385)$. The expression in square brackets describes the $\Sigma(1385)$ decay distribution in terms of the density matrix elements ρ_{33}, Re ρ_{31} and Re ρ_{3-1} which themselves are functions of production angle. Following the formalism set out by Deen [12] * the differential cross section and the density matrix elements for reactions (2) and (3) are expanded in

* We believe that the system of axes for the decay of the Λ from the Σ(1385) used in his report is inconsistent and we therefore use the following the **z** axis is along the direction of the Λ in the Σ(1385) rest frame, and the **y** axis is defined as $\mathbf{y} = (\mathbf{z}' \times \mathbf{z})/|(\mathbf{z}' \times \mathbf{z})|$ where $\mathbf{z}'$ is the direction of the Σ(1385) in the overall c m system

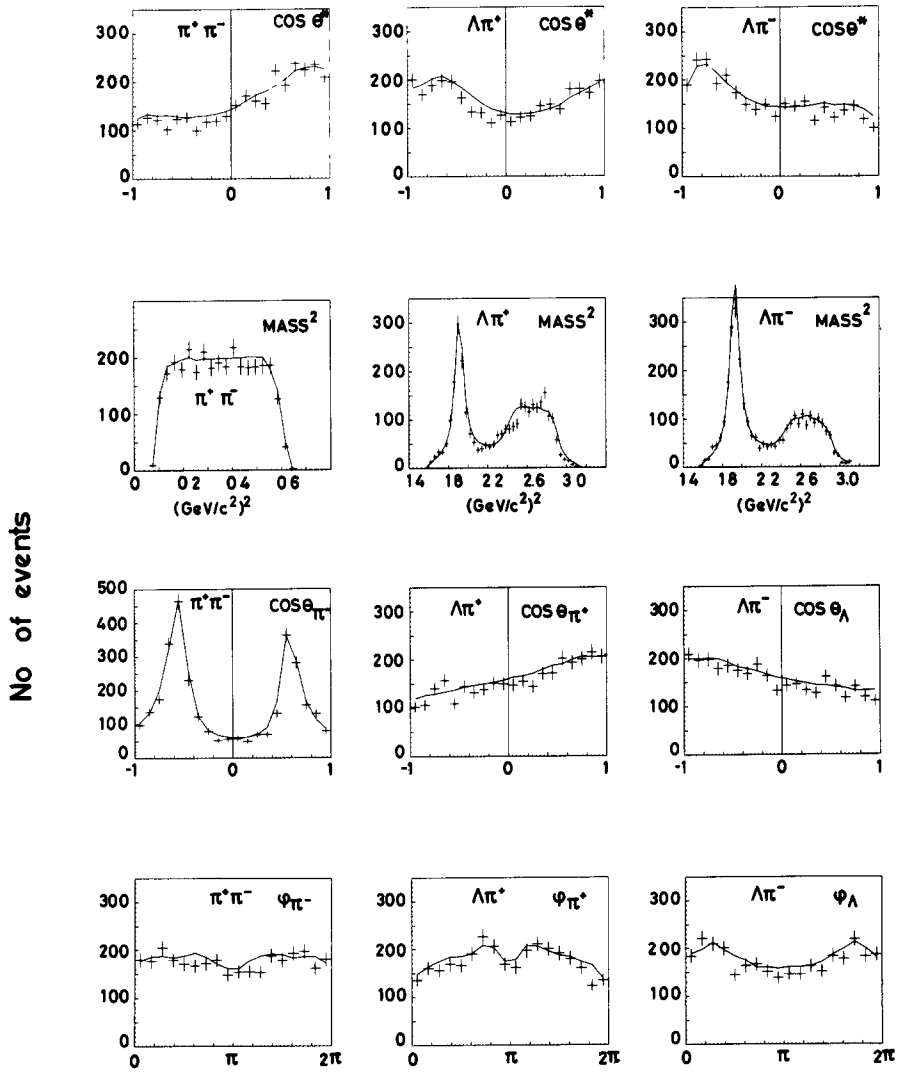

Fig. 5 The four one-variable distributions for each of the two-particle combinations at 1 245 GeV/c K^- incident momentum The curves were obtained by Monte Carlo integration using the fitted values of the A, B, C, D coefficients

Legendre polynomial series·

$$\frac{d\sigma}{d\cos\theta^*} = 2\pi\lambda^2 \sum_l A_l P_l^0(\cos\theta^*) , \tag{9}$$

Table 3
Values of the coefficients $A_0, A_l/A_0, B_l/A_0, C_l/A_0, D_l/A_0, E_l/A_0, F_l/A_0, G_l/A_0, H_l/A_0$ for $K^- p \to \pi^- \Sigma^+(1385)$

Table 3(a)

Beam momentum (GeV/c)	A0 * 100	A1/A0	A2/A0	A3/A0	A4/A0	A5/A0	A6/A0	A7/A0
0 960	6 68 ± 0 64	0 01 ± 0 10	0 05 ± 0 12	−0.49 ± 0 14	−0 44 ± 0 16	0.09 ± 0.18	−0 33 ± 0.19	0 21 ± 0 21
1 005	6 35 ± 0 67	0.07 ± 0 13	0.60 ± 0.15	−0 45 ± 0 18	−0 43 ± 0 20	−0 20 ± 0 23	0 04 ± 0.24	0.24 ± 0 26
1 045	7 75 ± 0 65	0 15 ± 0 10	0 89 ± 0.11	−0 66 ± 0.13	−0 70 ± 0.15	0 02 ± 0 17	−0 38 ± 0 19	0.16 ± 0 20
1 085	6 16 ± 0.57	0.21 ± 0 12	1.21 ± 0 13	−0 78 ± 0.17	−0 50 ± 0.20	−0 18 ± 0.22	0 11 ± 0 24	−0 40 ± 0.25
1 125	6 53 ± 0.57	0 26 ± 0 11	1 00 ± 0.13	−0 79 ± 0 15	−0 46 ± 0 18	−0 27 ± 0 20	0 01 ± 0 21	0 06 ± 0.23
1 165	6.64 ± 0.55	0 17 ± 0 10	0 85 ± 0.12	−0.56 ± 0.14	−0 46 ± 0 16	−0.00 ± 0 17	−0.08 ± 0 19	0 00 ± 0.21
1 205	6 42 ± 0 55	0 08 ± 0.10	0.74 ± 0 12	−0.61 ± 0 14	−0 44 ± 0 16	0.13 ± 0 18	−0 05 ± 0 19	−0 31 ± 0.21
1 245	6 92 ± 0 52	0 46 ± 0.09	0.64 ± 0 10	−0.41 ± 0 13	−0 47 ± 0 15	−0.07 ± 0 16	0 13 ± 0.17	0.18 ± 0 18
1 285	6 75 ± 0 49	0 30 ± 0.09	0 57 ± 0 10	−0 60 ± 0 12	−0 47 ± 0 14	0 07 ± 0.15	0 06 ± 0 17	−0 10 ± 0 18
1 320	6 77 ± 0.55	0 64 ± 0 09	0.37 ± 0.10	−0 49 ± 0 12	−0 85 ± 0 14	−0.38 ± 0.16	−0 43 ± 0 17	0 02 ± 0.19
1 355	6 41 ± 0 45	0 66 ± 0.08	0.73 ± 0.09	−0 52 ± 0.11	−0.72 ± 0 13	−0.22 ± 0 15	−0.10 ± 0 16	0 13 ± 0.17

Table 3(b)

Beam momentum (GeV/c)	B0/A0	B1/A0	B2/A0	B3/A0	B4/A0	B5/A0	B6/A0	B7/A0
0 960	0 27 ± 0.03	0.22 ± 0 06	−0.23 ± 0 07	−0 24 ± 0 08	−0 03 ± 0 10	0 05 ± 0 11	−0 10 ± 0.11	0.00 ± 0 12
1.005	0 19 ± 0 04	0 20 ± 0 07	−0 27 ± 0 09	−0 14 ± 0 11	−0 04 ± 0 12	−0.07 ± 0 14	−0 17 ± 0 15	−0 01 ± 0 16
1.045	0 22 ± 0 03	0 36 ± 0 06	−0 21 ± 0 07	−0.11 ± 0 08	−0 30 ± 0 10	0 05 ± 0 11	0 05 ± 0 12	0.02 ± 0 13
1.085	0 21 ± 0 03	0 41 ± 0 07	−0 06 ± 0.08	−0 18 ± 0 10	−0 31 ± 0 12	0 02 ± 0 13	−0 01 ± 0 14	−0.04 ± 0 15
1.125	0 24 ± 0 03	0 36 ± 0 07	−0 05 ± 0 08	−0 13 ± 0.10	−0 15 ± 0 11	−0 14 ± 0.12	−0 00 ± 0 13	0.03 ± 0 14
1.165	0 25 ± 0.03	0 32 ± 0 06	−0.18 ± 0.07	−0.25 ± 0 09	−0 33 ± 0 10	−0.11 ± 0.11	−0.12 ± 0 11	−0.04 ± 0.13
1 205	0.22 ± 0 03	0.31 ± 0.06	−0 05 ± 0.07	−0 20 ± 0.09	−0 22 ± 0 10	0.01 ± 0.11	−0 13 ± 0 12	0 12 ± 0 13
1 245	0 28 ± 0.03	0 36 ± 0 05	0 10 ± 0.06	−0.18 ± 0 08	−0 11 ± 0 09	−0 14 ± 0 10	−0 03 ± 0 10	0 13 ± 0 12
1 285	0 28 ± 0 03	0 30 ± 0.05	−0.06 ± 0 06	−0 23 ± 0 08	−0.12 ± 0 09	−0 03 ± 0 10	−0 04 ± 0 10	0 01 ± 0 11
1 320	0 35 ± 0 03	0 41 ± 0 06	0.07 ± 0 07	−0 22 ± 0 08	−0 27 ± 0.09	−0 17 ± 0.10	−0 28 ± 0 11	0 03 ± 0 12
1 355	0 34 ± 0 03	0 43 ± 0.05	0 08 ± 0 06	−0 17 ± 0 07	−0 24 ± 0 08	−0 14 ± 0 09	0.03 ± 0 10	−0 01 ± 0 11

Table 3(c)

Beam momentum (GeV/c)	C1/A0 * 100	C2/A0 * 100	C3/A0 * 100	C4/A0 * 100	C5/A0 * 100	C6/A0 * 100	C7/A0 * 100
0 960	10 15 ± 3 51	7.08 ± 2.87	−0 26 ± 2 36	−3.14 ± 2 04	1 41 ± 1 80	−0.62 ± 1 67	−0.17 ± 1 51
1.005	1 00 ± 3 41	5.39 ± 3 24	2 25 ± 2 69	−0 25 ± 2.21	3 40 ± 2 00	−1 65 ± 2 00	0 25 ± 1 82
1 045	5 22 ± 2 62	9 89 ± 2.58	5 83 ± 2 14	2 09 ± 1 81	−0 51 ± 1 62	−1 14 ± 1 47	0 69 ± 1 34
1 085	−0 01 ± 3 23	9 94 ± 3.29	−0 55 ± 2 77	2 24 ± 2 38	1 14 ± 2 19	2 24 ± 2 04	1 96 ± 1 92
1.125	0 90 ± 2 98	11 53 ± 2 95	6.01 ± 2.49	1 56 ± 2 14	2 91 ± 1.93	−2.89 ± 1 86	0 61 ± 1 83
1 165	−9 05 ± 2 74	10 44 ± 2.75	−2.06 ± 2 35	4 18 ± 2 05	0 81 ± 1 80	−0 78 ± 1 66	−1 75 ± 1 53
1 205	−7 37 ± 2 90	8 72 ± 2 79	−3.41 ± 2 33	5 19 ± 2 01	0.07 ± 1 82	1 45 ± 1 68	−0 54 ± 1.57
1.245	−7 04 ± 2 75	3 14 ± 2 53	−2 43 ± 2.01	3 22 ± 1 77	3 89 ± 1 59	−0 43 ± 1 43	−1.10 ± 1 36
1 285	−8 02 ± 2.70	−0.94 ± 2 42	−4 08 ± 1.90	3 08 ± 1 70	2 96 ± 1 54	1 10 ± 1 39	−0.76 ± 1 24
1.320	−2 58 ± 2 97	−1 69 ± 2 62	−4 09 ± 2.12	5 80 ± 1.74	−0 59 ± 1.53	1 37 ± 1 38	0 34 ± 1 29
1 355	−5 47 ± 2 56	−9.58 ± 2 36	−4 28 ± 1 87	2.34 ± 1 61	1 00 ± 1.44	1 77 ± 1.34	−0 48 ± 1 24

Table 3(d)

Beam momentum (GeV/c)	D2/A0 * 100	D3/A0 * 100	D4/A0 * 100	D5/A0 * 100	D6/A0 * 100	D7/A0 * 100
0 960	6 52 ± 1 58	1 60 ± 0 89	0.64 ± 0 59	0 49 ± 0 42	0 32 ± 0 31	−0 06 ± 0 25
1 005	7 53 ± 1 60	2 15 ± 1.01	1 94 ± 0 65	0 56 ± 0 47	−0 14 ± 0 36	−0.33 ± 0 29
1 045	5 53 ± 1 15	1 62 ± 0 79	2 07 ± 0 54	0 00 ± 0 39	0 44 ± 0.30	−0 14 ± 0 24
1 085	0 88 ± 1.25	1 93 ± 0 90	0 24 ± 0 61	0.54 ± 0 44	−0 30 ± 0 34	−0.05 ± 0 27
1 125	3 31 ± 1 26	3 03 ± 0 85	1 06 ± 0 58	0 30 ± 0 41	−0 19 ± 0.32	−0.33 ± 0 25
1.165	5 02 ± 1.19	3 21 ± 0 78	0.19 ± 0 52	0 18 ± 0 39	−0 39 ± 0 30	−0 01 ± 0 24
1 205	4 78 ± 1 27	2 40 ± 0 80	−0 72 ± 0 54	−0.33 ± 0 39	−0 43 ± 0 29	−0 05 ± 0 24
1 245	1 80 ± 1 12	1 71 ± 0 71	−0 36 ± 0.47	0 13 ± 0 34	−0 17 ± 0.26	−0 16 ± 0 21
1.285	0 81 ± 1.15	2.27 ± 0 71	−0 08 ± 0 46	0 09 ± 0 34	0.02 ± 0 26	0 08 ± 0.20
1 320	1 97 ± 1 27	1 27 ± 0 80	0 52 ± 0 54	−0 15 ± 0 38	−0.25 ± 0 28	0 18 ± 0 23
1 355	0 08 ± 1 02	0 79 ± 0 68	0 37 ± 0.45	0 31 ± 0 32	0 04 ± 0 24	0 02 ± 0.19

Table 3(e)

Beam momentum (GeV/c)	E1/A0 * 100	E2/A0 * 100	E3/A0 * 100	E4/A0 * 100	E5/A0 * 100	E6/A0 * 100	E7/A0 * 100
0.960	4 41 ± 12.15	−8 17 ± 9.89	0 59 ± 7 78	−0 85 ± 7 01	−2.79 ± 6.32	5 63 ± 5 56	−3 83 ± 5 23
1.005	11 80 ± 12.14	−3 00 ± 10 17	−4.95 ± 8 60	−5 39 ± 6 85	2 50 ± 6 14	4 84 ± 6 27	4 09 ± 6 02
1 045	−0 29 ± 9.69	−8 04 ± 8.84	−0 32 ± 7 26	0 02 ± 6.05	3 71 ± 5.39	3 34 ± 5 19	2 62 ± 4.86
1 085	−17 19 ± 11.72	−12.33 ± 11 32	−8 48 ± 9 17	6 80 ± 7 77	5.09 ± 7 23	−1 59 ± 6 73	−4.31 ± 6 13
1 125	−11 44 ± 11 47	−13 93 ± 10 53	1 20 ± 9 00	−6 10 ± 7 96	1.10 ± 7 51	−8 96 ± 6.99	3 28 ± 6 71
1 165	−14 96 ± 10 08	2 19 ± 9 58	−15 01 ± 8·20	11 62 ± 7 03	−8 35 ± 6 49	4 74 ± 5.51	−2 57 ± 4 99
1.205	−21 07 ± 11 02	−9 17 ± 10 69	−8 43 ± 8 91	7 31 ± 7.69	7 16 ± 6.87	4 56 ± 6 37	0 58 ± 6 00
1 245	−10 82 ± 10 14	−0 85 ± 9 28	5 08 ± 7 71	3.75 ± 6.74	7 58 ± 6 13	−7 08 ± 5 66	0 99 ± 5 15
1 285	−12 31 ± 10.32	−3 63 ± 8 83	1.95 ± 7 15	4 02 ± 6 36	4.01 ± 5.54	−4 50 ± 4.99	0 59 ± 4 72
1 320	−20 76 ± 11 42	−17 25 ± 10 02	−9.28 ± 8 21	−0.86 ± 6 50	5 88 ± 6 16	−0 95 ± 5.51	3 76 ± 4 91
1 355	−0 63 ± 10.27	1 53 ± 9 41	1 41 ± 7 49	−1 72 ± 6 43	0 58 ± 5 71	0 04 ± 5.20	4 36 ± 4.85

Table 3(f)

Beam momentum (GeV/c)	F2/A0 * 100	F3/A0 * 100	F4/A0 * 100	F5/A0 * 100	F6/A0 * 100	F7/A0 * 100
0 960	−5 07 ± 4 08	0 57 ± 2 27	−1 24 ± 1.52	1 19 ± 1.08	0.19 ± 0.78	0.11 ± 0.63
1.005	−4 99 ± 3 75	1 87 ± 2 38	0.33 ± 1 50	−1.01 ± 1 08	0.06 ± 0.82	0 06 ± 0.66
1 045	−3.30 ± 2.64	−0 45 ± 1 90	−1.07 ± 1.33	−0.18 ± 0 99	0 11 ± 0 77	0 37 ± 0 62
1.085	−2 06 ± 3 05	−0 96 ± 2 32	−2.08 ± 1.62	−0 57 ± 1.19	−0.27 ± 0 91	0.12 ± 0.70
1 125	−1.03 ± 2 85	0 46 ± 2 05	−1 93 ± 1 40	0 46 ± 1 01	−1 07 ± 0.75	0 26 ± 0.60
1 165	−5 25 ± 2 72	−1.13 ± 1 92	−2.13 ± 1.30	−0 41 ± 0 99	0 04 ± 0 76	−0.02 ± 0 60
1.205	−4 81 ± 2 87	0.14 ± 1.90	−1.71 ± 1 28	−0 55 ± 0 93	0.09 ± 0 70	0 05 ± 0 55
1.245	−3.06 ± 2 65	0 69 ± 1 68	−0.28 ± 1.10	−0.39 ± 0.78	−0 42 ± 0 62	−0.39 ± 0 49
1 285	−5 45 ± 2 73	−0 77 ± 1 75	−1 19 ± 1.13	0 09 ± 0.81	0 44 ± 0.61	−0 39 ± 0 48
1 320	−4 53 ± 2 78	0.94 ± 1 79	−1 53 ± 1 25	0.41 ± 0.89	−0 56 ± 0.65	−0.03 ± 0 51
1 355	−3 42 ± 2 31	−0 51 ± 1 56	−0.79 ± 1 06	0 40 ± 0 76	0 27 ± 0 57	0 64 ± 0 46

Table 3(g)

Beam momentum (GeV/c)	G1/A0 * 100	G2/A0 * 100	G3/A0 * 100	G4/A0 * 100	G5/A0 * 100	G6/A0 * 100	G7/A0 * 100
0 960	−17 67 ± 14.13	5 53 ± 13 32	−5 08 ± 10 71	9 10 ± 8 94	−0 56 ± 7.78	−1.27 ± 7 34	3.62 ± 6 75
1 005	−1 25 ± 13 73	−16 34 ± 14 27	7.09 ± 11.88	−2 24 ± 9 71	1 18 ± 9 13	−7.07 ± 9.35	−6.20 ± 9 11
1 045	−0.98 ± 10 08	−7 66 ± 11 05	−4 72 ± 9.92	1 11 ± 8 23	−0 79 ± 7.30	1 96 ± 7.24	−0.53 ± 6.98
1 085	10 62 ± 13 30	−15 40 ± 14 49	11 42 ± 12.22	−13 57 ± 10 17	3.03 ± 9.69	1.69 ± 8 95	−2.89 ± 8 09
1 125	5 56 ± 12 24	−0.09 ± 13 11	0 88 ± 11 78	3 10 ± 10 99	−0.48 ± 10 20	14.46 ± 9 53	−0 34 ± 9 28
1 165	15 56 ± 10 66	−17 04 ± 11 83	17.57 ± 10.84	−17.28 ± 9 58	8 70 ± 8.66	−3.32 ± 7.98	3.14 ± 7 18
1 205	13.95 ± 13.49	−4.31 ± 13 01	6 36 ± 10 92	−8 70 ± 9.98	−7 63 ± 9 09	−7.90 ± 8 38	−7 44 ± 8 07
1 245	5 76 ± 10.81	−4.98 ± 10.30	−0 82 ± 8 59	−1 48 ± 7 94	−9.09 ± 7.29	7 65 ± 6 60	−3.57 ± 5.64
1 285	1 90 ± 10 25	−1.19 ± 9 90	5 25 ± 7 96	−4.39 ± 6.82	−2 96 ± 6 30	2 15 ± 5 67	0.03 ± 5 22
1 320	14 49 ± 9 57	5 24 ± 9 12	7.16 ± 7 42	−3 11 ± 6 19	−5 95 ± 5.72	−0 57 ± 5 18	−3.70 ± 4 55
1.355	−7 53 ± 9 47	−2 25 ± 9 49	2 62 ± 7 79	5.46 ± 6 56	3.21 ± 5 99	5.00 ± 5.40	−3.62 ± 5.13

Table 3(h)

Beam momentum (GeV/c)	H3/A0 * 100	H4/A0 * 100	H5/A0 * 100	H6/A0 * 100	H7/A0 * 100
0.960	0 39 ± 1 13	−0 66 ± 0.49	−0 23 ± 0 27	−0.19 ± 0 17	0 08 ± 0 11
1.005	0.11 ± 1 08	−0.72 ± 0 51	−0 03 ± 0.30	−0.21 ± 0 19	0.06 ± 0 12
1 045	−0.87 ± 0 72	−0.30 ± 0 41	−0 14 ± 0.25	−0 05 ± 0 16	−0.04 ± 0.11
1.085	−1 03 ± 0 74	−0 51 ± 0 46	0 13 ± 0.28	0.01 ± 0.18	0.11 ± 0 12
1 125	−0 28 ± 0 76	0 03 ± 0.42	−0 25 ± 0 25	0 10 ± 0 16	−0 00 ± 0 11
1 165	−0.16 ± 0 77	0 05 ± 0 41	0 02 ± 0 23	0 08 ± 0 15	0.08 ± 0 11
1 205	−1.04 ± 0 80	−0 44 ± 0 43	−0 09 ± 0 24	0 09 ± 0 16	0 10 ± 0.11
1 245	−0.37 ± 0 71	−0 10 ± 0 37	0 17 ± 0.21	0 11 ± 0.13	−0.05 ± 0 09
1.285	−0.01 ± 0 69	−0.18 ± 0.35	−0 04 ± 0.20	−0 03 ± 0 13	−0 02 ± 0 09
1.320	−0.42 ± 0 82	−0.45 ± 0 41	0 17 ± 0 25	0.06 ± 0.15	0 03 ± 0 10
1 355	−0 13 ± 0 64	−0.51 ± 0 35	−0 02 ± 0 21	0.01 ± 0 13	0 05 ± 0.09

Table 4
As for table 3 for $K^- p \to \pi^+ \Sigma^-$ (1385)

Table 4(a)

Beam momentum (GeV/c)	A0 * 100	A1/A0	A2/A0	A3/A0	A4/A0	A5/A0	A6/A0	A7/A0
0.960	10.44 ± 0 91	−0 11 ± 0 08	−0 15 ± 0 09	0 39 ± 0 12	−0 60 ± 0 13	−0 09 ± 0 15	0 32 ± 0 17	0.00 ± 0 18
1 005	11.27 ± 1 05	0 14 ± 0 09	−0 06 ± 0 11	0 22 ± 0 13	−0 38 ± 0 14	−0 14 ± 0.16	−0 10 ± 0 18	−0 05 ± 0 19
1 045	12.31 ± 0 92	0 31 ± 0 07	0.30 ± 0 09	0 43 ± 0 11	−0 30 ± 0 12	−0 51 ± 0.14	−0 03 ± 0 15	−0 08 ± 0 16
1 085	12 01 ± 0 96	0.55 ± 0 08	0 31 ± 0 09	0 22 ± 0 11	−0.42 ± 0.13	−0.07 ± 0 14	0 06 ± 0 16	0.19 ± 0 17
1.125	11.69 ± 0 88	0 56 ± 0 08	0 36 ± 0 09	−0 05 ± 0 11	−0 42 ± 0 12	−0.13 ± 0 14	−0 10 ± 0 15	0 08 ± 0.16
1 165	10 76 ± 0 79	0 61 ± 0 07	0 24 ± 0 09	0 10 ± 0 11	−0 42 ± 0 12	−0 40 ± 0.13	−0.10 ± 0 15	−0.13 ± 0 16
1 205	10 44 ± 0 80	0 77 ± 0 07	0 26 ± 0 09	−0 25 ± 0 11	−0 45 ± 0 12	−0.28 ± 0 13	−0 09 ± 0 15	−0.03 ± 0 17
1 245	9 58 ± 0 67	0 74 ± 0 07	0 27 ± 0.08	−0.04 ± 0 10	−0 58 ± 0.11	−0 35 ± 0 13	−0.24 ± 0 14	−0 03 ± 0 15
1 285	8 73 ± 0.59	0 82 ± 0 07	0 30 ± 0 08	−0 13 ± 0 10	−0.59 ± 0 12	−0 20 ± 0 13	0 01 ± 0 15	−0 14 ± 0 15
1 320	8 54 ± 0 66	0 82 ± 0 09	0 75 ± 0 10	−0 09 ± 0 11	−0 74 ± 0 13	−0 37 ± 0 15	−0 48 ± 0.16	−0 14 ± 0 17
1 355	7 78 ± 0 52	0 69 ± 0 07	0 58 ± 0 08	−0 20 ± 0 10	−0 62 ± 0 12	−0 18 ± 0 13	−0 31 ± 0 14	−0.11 ± 0 15

Table 4(b)

Beam momentum (GeV/c)	B0/A0	B1/A0	B2/A0	B3/A0	B4/A0	B5/A0	B6/A0	B7/A0
0 960	0.26 ± 0 03	−0 19 ± 0 05	−0 10 ± 0 06	0 20 ± 0 08	−0.25 ± 0.08	−0.05 ± 0 09	0 11 ± 0 10	−0.02 ± 0 11
1 005	0 29 ± 0 03	−0 16 ± 0 05	−0 21 ± 0 06	0 08 ± 0 08	−0 16 ± 0 09	0 08 ± 0 10	0 03 ± 0 11	0 09 ± 0 12
1 045	0 25 ± 0 02	−0 06 ± 0 04	−0 08 ± 0 06	0 13 ± 0 07	−0 03 ± 0.08	−0.17 ± 0 08	−0 06 ± 0 09	0 11 ± 0.10
1 085	0 21 ± 0 03	−0 04 ± 0.05	−0 18 ± 0 06	0 02 ± 0 07	0 02 ± 0 08	0 19 ± 0 08	0 01 ± 0 09	−0 02 ± 0 10
1 125	0 23 ± 0 03	−0 11 ± 0 05	−0 10 ± 0 06	−0 06 ± 0.07	0 05 ± 0 08	0 10 ± 0 09	0 06 ± 0.10	0 08 ± 0 10
1 165	0 27 ± 0 02	−0 03 ± 0 05	−0 24 ± 0 05	−0 09 ± 0 07	0 02 ± 0 07	−0 00 ± 0 08	0 06 ± 0 09	0.00 ± 0 10
1 205	0 27 ± 0 02	0 07 ± 0 05	−0 13 ± 0 06	−0 18 ± 0 07	−0.06 ± 0 08	−0 12 ± 0 08	0 01 ± 0 09	0.04 ± 0.10
1 245	0 23 ± 0 02	0 10 ± 0 04	−0 10 ± 0 05	−0 11 ± 0 06	−0 08 ± 0 07	−0 13 ± 0 08	0 03 ± 0 09	0 02 ± 0 09
1 285	0 23 ± 0 02	0 14 ± 0 04	−0 08 ± 0 05	−0 14 ± 0 06	−0 13 ± 0 07	−0 07 ± 0 08	−0 02 ± 0 09	0 03 ± 0 09
1 320	0 22 ± 0 03	0 09 ± 0 05	−0 05 ± 0 06	−0 08 ± 0 07	−0 17 ± 0 08	−0 11 ± 0 09	−0 10 ± 0 10	−0 10 ± 0 10
1 355	0 25 ± 0 02	0 07 ± 0 04	−0 07 ± 0 05	−0 18 ± 0 06	−0 11 ± 0 07	0 02 ± 0 08	−0 03 ± 0 08	−0 03 ± 0 09

Table 4(c)

Beam momentum (GeV/c)	C1/A0 * 100	C2/A0 * 100	C3/A0 * 100	C4/A0 * 100	C5/A0 * 100	C6/A0 * 100	C7/A0 * 100
0 960	6 71 ± 2 95	0 58 ± 2 35	−3 14 ± 1 85	−1 58 ± 1.68	0 08 ± 1.48	−0 40 ± 1.31	−0 11 ± 1 21
1 005	8 63 ± 3 02	1 47 ± 2 44	1.41 ± 2.07	0 46 ± 1 77	−0.46 ± 1 57	2 17 ± 1 44	−0 79 ± 1 36
1 045	9 67 ± 2 50	0 59 ± 2 12	0 69 ± 1.67	−1 20 ± 1 44	−4 06 ± 1 30	−1.57 ± 1 23	−0 51 ± 1.12
1 085	9 64 ± 2 59	1 48 ± 2 21	1 05 ± 1 74	1.14 ± 1 57	−0 68 ± 1.40	0.65 ± 1 31	−0 02 ± 1.25
1 125	10.01 ± 2.53	0 16 ± 2 16	0 03 ± 1.73	−1 54 ± 1 52	−1.39 ± 1.33	−0 76 ± 1 23	−1 56 ± 1 16
1 165	9 79 ± 2 49	2 22 ± 2 14	3.00 ± 1 71	−2 13 ± 1.47	−2.15 ± 1 32	0 37 ± 1 20	0 72 ± 1.11
1 205	14 49 ± 2 59	5 41 ± 2 18	3.40 ± 1 72	−1 57 ± 1 52	−2 36 ± 1 36	−0 55 ± 1 21	0 88 ± 1 11
1 245	18 82 ± 2 49	7.09 ± 2 10	3.61 ± 1 70	−1.03 ± 1.45	−1 34 ± 1 29	−0 67 ± 1 16	−0 01 ± 1.09
1 285	14 52 ± 2 50	13 80 ± 2.12	3 68 ± 1 66	−4 08 ± 1.49	−2 66 ± 1 29	−1 68 ± 1 18	−0 12 ± 1 13
1 320	12 97 ± 2 66	16 42 ± 2 48	4 26 ± 2 08	−1 60 ± 1 77	−2 63 ± 1 56	−2 50 ± 1 46	0 17 ± 1 33
1 355	9 14 ± 2 39	13 08 ± 2 19	2 30 ± 1 82	−0.57 ± 1 57	−3 69 ± 1.38	−2 48 ± 1.24	0 34 ± 1.18

Table 4(d)

Beam momentum (GeV/c)	D2/A0 * 100	D3/A0 * 100	D4/A0 * 100	D5/A0 * 100	D6/A0 * 100	D7/A0 * 100
0.960	7 29 ± 1 38	−0 22 ± 0.79	0.49 ± 0.48	0.49 ± 0 34	−0 32 ± 0.27	−0.00 ± 0.21
1.005	6 45 ± 1 40	0 18 ± 0 77	0 36 ± 0 50	−0 14 ± 0 36	−0 29 ± 0.27	0 12 ± 0.21
1.045	5 13 ± 1.08	0.95 ± 0.63	0.32 ± 0 42	0 33 ± 0 30	0 59 ± 0.23	0 23 ± 0 18
1 085	3 99 ± 1 12	0 30 ± 0 65	0 62 ± 0.43	0 55 ± 0 30	0 38 ± 0 24	−0.07 ± 0 19
1.125	5 14 ± 1.12	1.08 ± 0.66	1.05 ± 0 44	0 70 ± 0 32	0.23 ± 0 24	−0.04 ± 0.19
1 165	3 62 ± 1.10	0 55 ± 0.64	0.63 ± 0 42	0 32 ± 0.30	0 07 ± 0.23	0.21 ± 0.18
1 205	3 96 ± 1.12	0 53 ± 0.66	0.34 ± 0 42	0 20 ± 0 30	0.32 ± 0 23	−0.05 ± 0 19
1 245	2 46 ± 1 03	−0 51 ± 0.62	0 59 ± 0.41	0.30 ± 0.29	0 24 ± 0 22	0.04 ± 0 17
1.285	3.93 ± 1 06	−0 50 ± 0.65	0 79 ± 0.42	0 20 ± 0 30	0 21 ± 0 22	0.05 ± 0 17
1 320	3 24 ± 1 09	−0 34 ± 0.72	1.13 ± 0.49	0 50 ± 0 35	0.15 ± 0 26	−0 28 ± 0 20
1.355	2 72 ± 0.97	−1 13 ± 0.62	0 94 ± 0 42	−0 19 ± 0 29	0 10 ± 0 22	−0 07 ± 0 18

Table 4(e)

Beam momentum (GeV/c)	E1/A0 * 100	E2/A0 * 100	E3/A0 * 100	E4/A0 * 100	E5/A0 * 100	E6/A0 * 100	E7/A0 * 100
0.960	−6.68 ± 11 41	−0 10 ± 8 64	4.33 ± 6.55	−4 53 ± 5 95	2 37 ± 5 45	3.09 ± 4.76	−1.98 ± 4.33
1.005	−12 30 ± 11 29	−1.50 ± 8.73	0.30 ± 7 35	−5 83 ± 6 59	3 10 ± 5 36	0.09 ± 4.78	−7 03 ± 4 63
1.045	−10 86 ± 8.64	−0 55 ± 7 07	5.78 ± 5 58	−1 94 ± 4.95	1 23 ± 4.44	−0.53 ± 4 11	4 31 ± 3.94
1 085	−9.85 ± 9.36	−0 32 ± 7 48	−8.53 ± 5.97	−4 68 ± 5 40	0.30 ± 4.93	−0 58 ± 4.45	−0.41 ± 4.31
1 125	−5.54 ± 9 05	−4.32 ± 7 44	5 48 ± 6 26	−8 53 ± 5.40	2 70 ± 4.89	−5 16 ± 4.52	−2 23 ± 4.32
1 165	−9 41 ± 9.89	−7 82 ± 7.51	−1 57 ± 6 36	−5 52 ± 5 27	−0 70 ± 4 76	0.43 ± 4.31	0 10 ± 4.12
1 205	−7.34 ± 9 12	−3 44 ± 7 64	1.40 ± 6 08	−1.93 ± 5.27	6 88 ± 4 79	3 42 ± 4.18	2 84 ± 3.87
1 245	−3 91 ± 9 15	10 24 ± 7 82	−3 35 ± 5 96	−3 75 ± 4 97	−0 44 ± 4 72	−0 79 ± 4 17	0 32 ± 3.76
1 285	−4 74 ± 9.10	1 22 ± 7 40	2.07 ± 5.89	2 57 ± 4.85	−1 52 ± 4.39	−4 09 ± 4 04	−5.04 ± 3.82
1 320	−3 01 ± 9.60	−0 88 ± 8 60	−5 83 ± 7.08	−2.57 ± 5.85	1 29 ± 5.13	3.78 ± 4.63	3.74 ± 4.40
1.355	4 97 ± 8 72	7.34 ± 7.27	0 84 ± 6 01	−5 04 ± 5 14	1.02 ± 4 68	−0.51 ± 4.17	−3 02 ± 4.00

Table 4(f)

Beam momentum (GeV/c)	F2/A0 * 100	F3/A0 * 100	F4/A0 * 100	F5/A0 * 100	F6/A0 * 100	F7/A0 * 100
0 960	4 95 ± 3 45	−0 27 ± 1 91	−0 90 ± 1 22	−0 56 ± 0 86	−0 22 ± 0 69	0 01 ± 0 54
1.005	2 53 ± 3 49	−1 99 ± 1 96	0 47 ± 1 29	0 29 ± 0 92	0 36 ± 0 68	0 51 ± 0 54
1 045	1 68 ± 2 61	1 54 ± 1.56	2 37 ± 1.04	0 33 ± 0 73	0.22 ± 0 54	−0 11 ± 0 43
1 085	3 31 ± 2 76	−0 04 ± 1 66	0 91 ± 1 07	−0.23 ± 0 75	0 01 ± 0 59	−0.32 ± 0.46
1.125	3 30 ± 2 75	1.69 ± 1 61	0 53 ± 1 04	−0.37 ± 0 75	0 42 ± 0 55	0 24 ± 0.46
1 165	3 10 ± 2 64	1 21 ± 1 60	0 83 ± 1.06	0 29 ± 0 73	0 26 ± 0 56	−0.25 ± 0 45
1 205	2 61 ± 2 71	2 22 ± 1.59	1.92 ± 1 04	0 40 ± 0 74	−0.01 ± 0 58	−0 09 ± 0 47
1 245	3 43 ± 2 58	3 13 ± 1.57	2.29 ± 1.04	0 44 ± 0 73	0 25 ± 0 55	0 11 ± 0.44
1.285	2.64 ± 2.55	3.19 ± 1.58	1.06 ± 1.03	0.26 ± 0.75	0 15 ± 0.57	0.23 ± 0.44
1 320	1 31 ± 2 67	5 39 ± 1 84	1 69 ± 1 26	1 00 ± 0 90	0.37 ± 0 65	−0.34 ± 0.51
1 355	0 93 ± 2 32	4 59 ± 1 55	1 06 ± 1 04	0 34 ± 0 73	0 38 ± 0.57	−0 37 ± 0 47

Table 4(g)

Beam momentum (GeV/c)	G1/A0 * 100	G2/A0 * 100	G3/A0 * 100	G4/A0 * 100	G5/A0 * 100	G6/A0 * 100	G7/A0 * 100
0 960	21.63 ± 13 98	−4 21 ± 10.37	−7 27 ± 8.41	1 88 ± 7 47	−5 98 ± 6.80	−3 37 ± 6.22	0 18 ± 5 69
1.005	10 82 ± 11 73	−5 59 ± 10 64	5.89 ± 9 41	4 41 ± 7 94	2 31 ± 6 60	0 62 ± 6 08	1 86 ± 5 82
1 045	8 28 ± 10 52	−11 18 ± 9 25	−1.71 ± 7 15	1 03 ± 6 02	−11 05 ± 5.41	1 51 ± 5 07	−2 71 ± 4 85
1.085	23 59 ± 10 99	4.86 ± 9 95	16 73 ± 7 80	4 74 ± 7 28	2.07 ± 6 69	0 01 ± 6.21	3.17 ± 5 95
1 125	4 37 ± 10 81	−3 26 ± 10 11	−8.61 ± 8.22	2 30 ± 7 24	−1 93 ± 6 34	2 22 ± 5 90	3 50 ± 5 78
1 165	10 81 ± 10 27	−1.04 ± 9 73	6 40 ± 8 07	2 75 ± 6 66	−0 50 ± 5 91	0 68 ± 5.58	1 46 ± 5 40
1 205	−1 46 ± 10 28	−9.21 ± 9 24	0.99 ± 7 69	1 38 ± 7 02	−7 06 ± 6 10	−8 59 ± 5 20	−4 69 ± 4.58
1.245	4 09 ± 11 08	−11 90 ± 10 08	4 39 ± 7 78	0 91 ± 6 34	−0.56 ± 5 94	−0 46 ± 5 40	0 70 ± 4.91
1 285	9 91 ± 11 08	8 73 ± 9 74	0 71 ± 7 52	−1 53 ± 6 52	8 28 ± 5 69	6 12 ± 5 46	7 93 ± 5 17
1 320	17 72 ± 10 36	7 12 ± 10 68	15 96 ± 9 06	2 51 ± 7 50	0 69 ± 6 35	1.09 ± 6.15	−4 77 ± 6 05
1 355	−0.51 ± 9 15	−4.36 ± 9 09	−8.15 ± 7 68	−0.70 ± 6 77	−6 84 ± 6 10	−1 34 ± 5.24	3.36 ± 5 01

Table 4(h)

Beam momentum (GeV/c)	H3/A0 * 100	H4/A0 * 100	H5/A0 * 100	H6/A0 * 100	H7/A0 * 100
0 960	−2 48 ± 0 94	0 22 ± 0 43	−0 23 ± 0 22	−0 08 ± 0 14	−0.01 ± 0.09
1 005	−1 41 ± 0 92	0 18 ± 0.41	−0.39 ± 0 22	0 02 ± 0 14	0 02 ± 0 10
1.045	−2 01 ± 0 74	−0 34 ± 0.34	0.02 ± 0 20	−0.04 ± 0 12	0 01 ± 0 08
1 085	−1 82 ± 0 74	−0 04 ± 0.35	0 07 ± 0.20	0 19 ± 0 12	−0.05 ± 0 08
1 125	−2 45 ± 0 70	−0 24 ± 0 33	−0.09 ± 0 19	0.03 ± 0 12	0 12 ± 0 08
1 165	−2 17 ± 0 75	−0 42 ± 0 35	−0 17 ± 0 20	0 11 ± 0 12	0 06 ± 0.08
1 205	−1 67 ± 0 73	−0 30 ± 0.35	−0 12 ± 0.19	−0 00 ± 0 12	0 02 ± 0 08
1 245	−1 41 ± 0 67	−0 51 ± 0.32	−0 26 ± 0.19	−0 14 ± 0 12	−0 11 ± 0 08
1 285	−1 88 ± 0 69	−0 44 ± 0 34	−0 15 ± 0 19	0 10 ± 0 12	0 04 ± 0.08
1 320	−0 77 ± 0 68	−0 37 ± 0 37	−0 20 ± 0.22	−0 14 ± 0 14	−0 03 ± 0.09
1 355	−1.03 ± 0 62	−0 29 ± 0 31	−0 19 ± 0.18	−0 00 ± 0 11	−0 01 ± 0 08

$$\rho_{33}\frac{d\sigma}{d\cos\theta^*} = 2\pi\lambda\bar{}^2 \sum_l B_l P_l^0(\cos\theta^*) ,$$

$$\mathrm{Re}\,\rho_{31}\frac{d\sigma}{d\cos\theta^*} = 2\pi\lambda\bar{}^2 \sum_l C_l P_l^1(\cos\theta^*) ,$$

$$\mathrm{Re}\,\rho_{3-1}\frac{d\sigma}{d\cos\theta^*} = 2\pi\lambda\bar{}^2 \sum_l D_l P_l^2(\cos\theta^*) ,$$

Similar expansions were used for reaction (7). For all reactions the highest value of l used was 7.

The expansion coefficients extracted by this procedure were checked against the results of the moments programme developed by Litchfield [13]. The results from the two methods were found to be in satisfactory agreement.

Data from the parity violating decay of the Λ were used together with the results of the above extraction to determine the remaining four independent elements of the density matrix ($\mathrm{Im}\,\rho_{31}$, $\mathrm{Im}\,\rho_{3-1}$, $\mathrm{Im}\,\rho_{1-1}$, $\mathrm{Im}\,\rho_{3-3}$). These elements were again expanded in Legendre polynomial series.

$$\mathrm{Im}\,\rho_{31}\frac{d\sigma}{d\cos\theta^*} = 2\pi\lambda\bar{}^2 \sum_l E_l P_l^1(\cos\theta^*) ,$$

$$\mathrm{Im}\,\rho_{3-1}\frac{d\sigma}{d\cos\theta^*} = 2\pi\lambda\bar{}^2 \sum_l F_l P_l^2(\cos\theta^*) ,$$

$$\mathrm{Im}\,\rho_{1-1}\frac{d\sigma}{d\cos\theta^*} = 2\pi\lambda\bar{}^2 \sum_l G_l P_l^1(\cos\theta^*) ,$$

$$\mathrm{Im}\,\rho_{3-3}\frac{d\sigma}{d\cos\theta^*} = 2\pi\lambda\bar{}^2 \sum_l H_l P_l^3(\cos\theta^*) , \qquad (10)$$

and the coefficients E_l, F_l, G_l and H_l (later referred to as polarisation coefficients) up to order 7 were calculated by the orthogonal moments method [12]

The complete set of coefficients for reactions (2) and (3) are given in tables 3 and 4 and some of the more significant coefficients are shown in figs. 6 and 7 together with data from the CRSS [14] * collaboration.

4. Partial-wave analysis

There is substantial overlap between the data from the CRSS collaboration [1] and those from this experiment Following our previous practice [15], we have

* Data summary tapes for the reaction $K^- p \to \Lambda\pi^+\pi^-$ were made available to us by the CRSS Collaboration These were analysed using the methods described for the present data

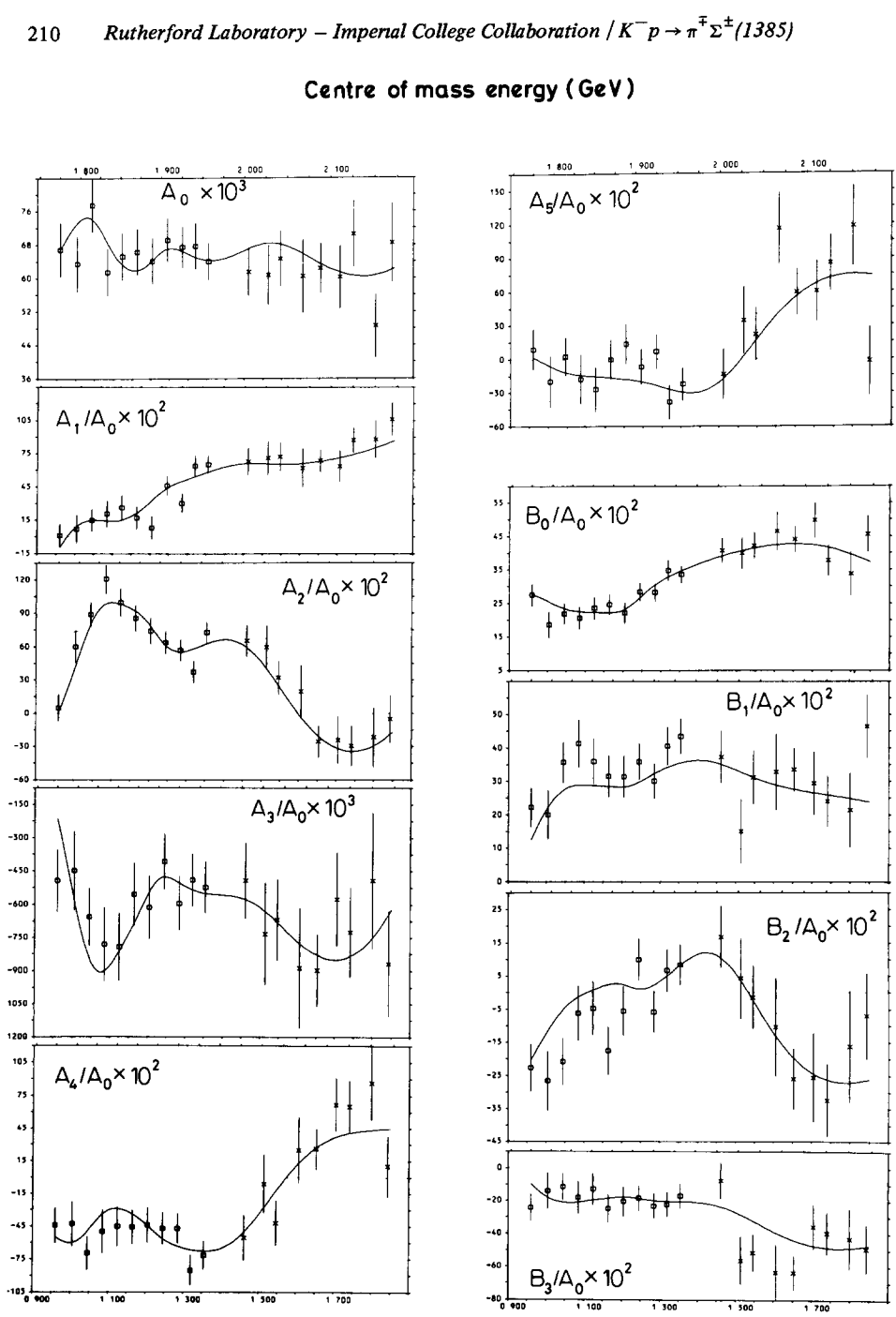
Centre of mass energy (GeV)
A0 ×10³
A1/A0× 10²
A2/A0× 10²
A3/A0× 10³
A4/A0× 10²
A5/A0× 10²
B0/A0× 10²
B1/A0× 10²
B2/A0× 10²
B3/A0× 10²
1 800
1 900
2 000
2 100
0 900
1 100
1 300
1 500
1 700
Incident K⁻momentum (GeV/c) →

Fig. 6a.

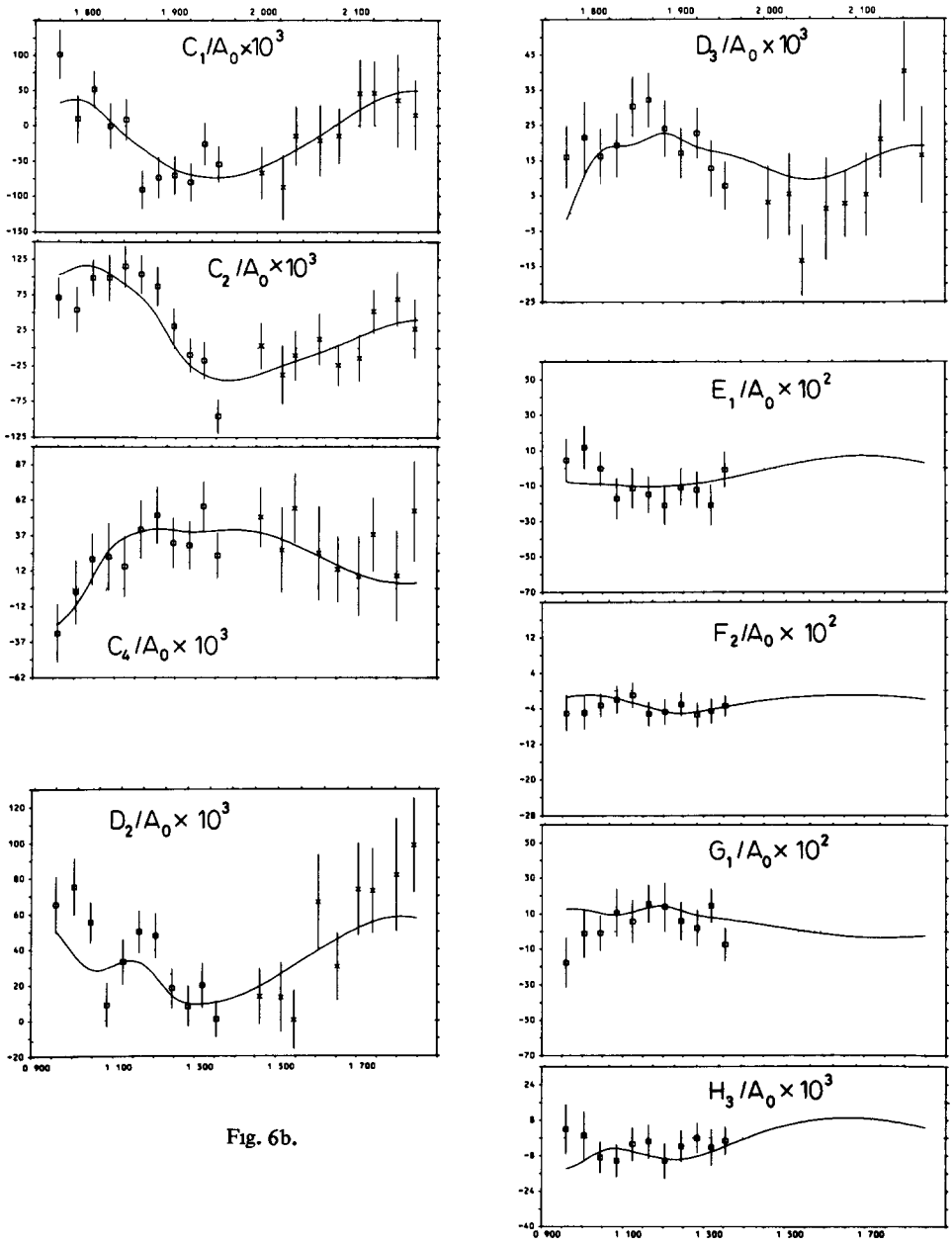

Fig. 6b.

Fig. 6 The most significant Legendre polynomial expansion coefficients for $K^- p \to \pi^- \Sigma^+(1385)$. The curve is the result of the partial-wave analysis. The data from the present experiment are shown as □, while the CRSS data are shown as ×

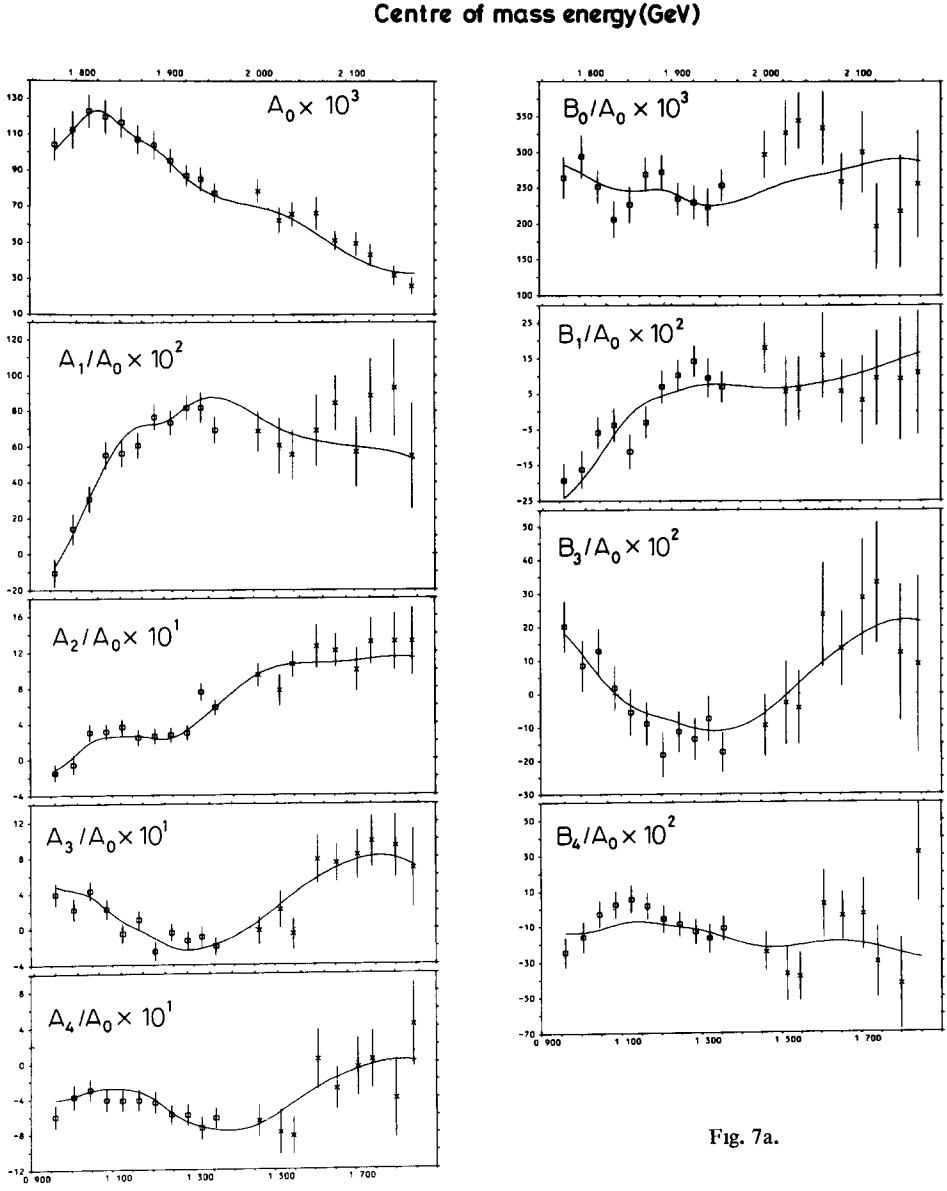
Centre of mass energy(GeV)
1 800
1 900
2 000
2 100
$A_0 \times 10^3$
$A_1/A_0 \times 10^2$
$A_2/A_0 \times 10^1$
$A_3/A_0 \times 10^1$
$A_4/A_0 \times 10^1$
$B_0/A_0 \times 10^3$
$B_1/A_0 \times 10^2$
$B_3/A_0 \times 10^2$
$B_4/A_0 \times 10^2$
0 900
1 100
1 300
1 500
1 700
Incident K^- momentum (GeV/c) ⟶

Fig. 7a.

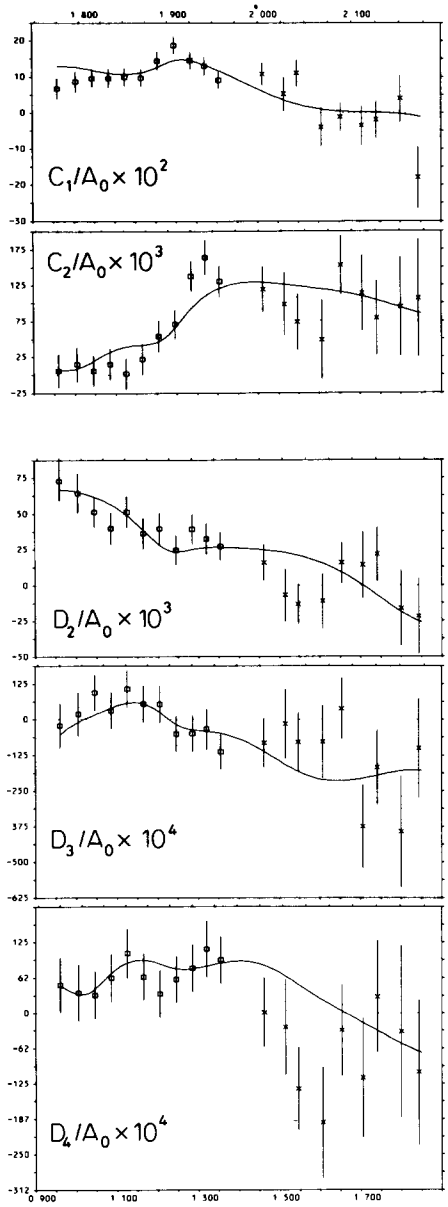

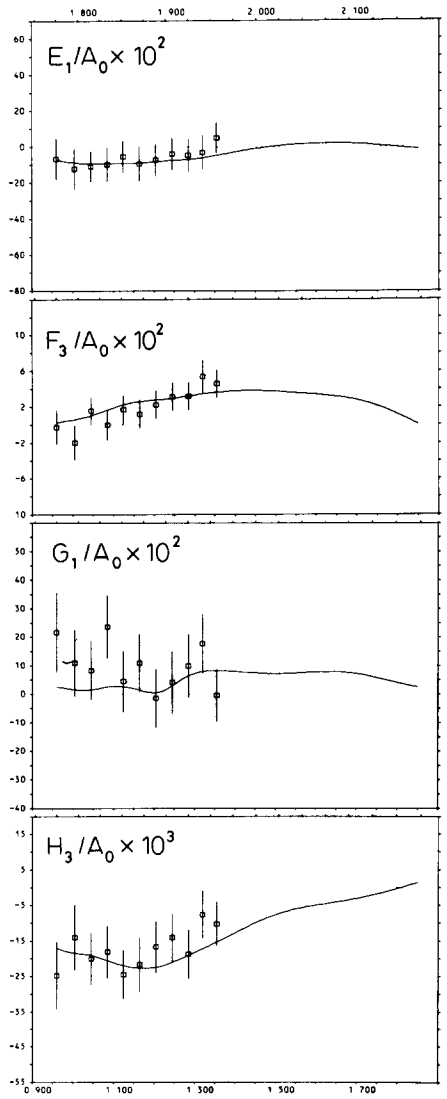

Fig. 7b.

Incident K^- momentum (GeV/c) →

Fig 7 As for fig 6, but for $K^-p \to \pi^+\Sigma^-(1385)$

Table 5
The data used in this analysis and the χ^2 contribution of each set given as χ^2 per data point

Momentum range (GeV/c)	c m Energy range (MeV)	Experiment	No of momenta	Type of data	No (N) of data points		χ^2/N	
					$\pi^-\Sigma^+$	$\pi^+\Sigma^-$	$\pi^-\Sigma^+$	$\pi^+\Sigma^-$
0.960–1 355	1775–1957	This expt	11	$A_0, A_I/A_0$	88	88	0 93	0.81
				B_I/A_0	88	88	0.84	0.89
				C_I/A_0	77	77	1.18	0 84
				D_I/A_0	66	66	1 06	0 59
				E_I/A_0	77	77	0 63	0 40
				F_I/A_0	66	66	0 34	0.36
				G_I/A_0	77	77	0 53	0 70
				H_I/A_0	55	55	0 49	0 47
1 462–1 843	2005–2170	CRSS (1)	9	$A_0, A_I/A_0$	72	72	0 87	0 78
				B_I/A_0	72	72	1 00	0 95
				C_I/A_0	63	63	0 90	0 88
				D_I/A_0	54	54	0 95	1 13

Total no of parameters = 62, no. of data points = 1710, χ^2/N = 0.78.

used data from the present higher-statistics experiment in the region of overlap. The data employed in the present partial wave analysis are listed in table 5.

4.1. The parametrisation

A partial-wave amplitude $T_{LL'I2J}$, where L and L' are the incoming and outgoing orbital angular momenta, I is the isotopic spin and J is the total angular momentum, is parametrised as a sum of a background term and, if required, Breit-Wigner terms:

$$T = T_B + T_R \,, \tag{11}$$

where T_B is the background term and T_R is a sum of non-relativistic Breit-Wigner resonances of the form

$$\frac{t}{\epsilon - i}\, e^{i\phi} \,, \tag{12}$$

where t is the resonance amplitude and $\epsilon = 2(E_R - E)/\Gamma(E)$. The energy-dependent width Γ is of the form.

$$\Gamma(E) = \Gamma(E_R)\frac{kv_l(kr)}{k_R v_l(k_R r)}\frac{E_R}{E} \,, \tag{13}$$

where v_l is the Blatt and Weisskopf angular momentum barrier [16] for the incoming orbital angular momentum l. The radius of interaction, r, is taken to be 1 fm In these formulae E and k are the c.m. energy and momentum and E_R and k_R are their

values at the resonance energy and

$$t = \sqrt{xx'} = \sqrt{\Gamma_e\Gamma_i/\Gamma^2} ,$$

Γ_e and Γ_i being the partial widths of the elastic and the $\pi\Sigma(1385)$ channel. The energy dependence of the elastic partial width was assumed to be the same as that of the total width. For Γ_i, k and k_R in the formula correspond to the c.m. momenta of the outgoing particles and l refers to the outgoing orbital angular momentum. It should be pointed out that the specific form assumed for the energy dependence of the widths does not affect the results significantly.

The background term has the form

$$T_B = \sqrt{B_l B_{l'}}\, R(E)\, e^{i\theta(E)} , \tag{14}$$

where

$$R(E) = \sum_{m=0}^{M} a_m P_m(E') , \qquad \theta(E) = \sum_{n=0}^{N} b_n P_n(E') ,$$

$$E' = \frac{2E - E_{max} - E_{min}}{E_{max} - E_{min}} ,$$

such that E' equals +1 and −1 at energies E_{max} and E_{min} just above the upper end and below the lower end of the energy range fitted, and P_m, P_n are Legendre polynomials. The parameters a_m and b_n are determined by fitting. The angular momentum barrier factor B_l has the form

$$B_l = \frac{k}{k_{max}} \frac{E_{max}}{E} \frac{v_l(kr)}{v_l(k_{max}r)} . \tag{15}$$

The various expansion coefficients of eqs. (9) and (10) may be related to the partial-wave amplitudes by

$$\eta_l = \sum_{L_1 L_1' I_1 J_1} \sum_{L_2 L_2' I_2 J_2} x^{L_2 L_2' I_2 J_2}_{L_1 L_1' I_1 J_1} \mathrm{PART}(T^*_{L_1 L_1' I_1 J_1} T_{L_2 L_2' I_2 J_2}) , \tag{16}$$

where η_l is any of the coefficients $A_l - H_l$, x's are the quasi two-body equivalent of the Tripp coefficients [17], and PART stands for Re (*ABCD* coefficients) or Im (*EFGH* coefficients).

4.2 The partial-wave solution

Several partial-wave solutions were developed starting from different assumptions about the presence of backgrounds and the less well established resonant states. However, the significant partial-wave amplitudes obtained were found to be essentially similar in all solutions [18] and so only the solution obtained with the minimum number of free parameters is described here.

Within the energy range 1775–2170 MeV there are three established $I = 1$ states, D15(1775), F15(1920), F17(2040) and four $I = 0$ states, P03(1900), D05(1830), F05(1820) and G07(2110) An initial basic solution was developed with these resonances and no background amplitudes in any of the partial waves. The masses and widths were fixed to the values found in the partial-wave analysis of two-body channels, ref. [15]. The resonant amplitudes were constrained to be purely imaginary at the resonant mass This solution gave a χ^2 of 5362 for 1696 degrees of freedom

At this stage the less well established resonances S11(1775), S11(1955), P01(1853) and S01(1825), D13(1920), F05(2100), G09(1808) reported in ref. [15] were added. Again the masses and widths were fixed and the amplitudes constrained to be purely imaginary at the resonant masses. After refitting, this solution gave a χ^2 of 3358 for 1687 degrees of freedom.

In order to improve the fit, background amplitudes were then introduced. This was done iteratively. In the first iteration two-parameter backgrounds ($N = M = 0$) see eq. (14)) were tried in each wave in turn and retained for that wave which gave the largest improvement in χ^2. The second iteration permitted either a second wave to carry $N = M = 0$ background or an increase in order of the background already found. This process of iteration was continued until there was no further significant improvement in χ^2

Background amplitudes were found necessary for waves with $J \leqslant \frac{5}{2}$ with the exception of SD01, FP05, FF05 and none were necessary for the higher waves This solution gave a χ^2 of 1289 for 1636 degrees of freedom

In order to investigate the significance of the 'less well established' resonances, this solution was re-minimised with each resonant amplitude removed in turn. Only those resonant amplitudes which lead to a change in χ^2 of more than 10 units were retained in the final solution These were the SD01(1825), FP05(2100), FF05(2100) and the DS13(1920) amplitudes

Using the same criterion for the established resonances, the amplitudes FP15(1920), FF15(1920), FH17(2040), GD07(2110) and the GG07(2110) were removed. However, the F15 wave was then dominated by a highly structured four-parameter background amplitude exhibiting a significant loop in the argand diagram suggesting a resonance of mass around 1900 MeV It was possible, quite satisfactorily, to replace this background by a two-parameter background and an F15 resonance, presumably the F15(1920), but the mass and width had to be changed to the values given in table 6. It should be noted however, that these values are in fact within the range permitted by the errors quoted in ref. [15] This solution has a χ^2 of 1326 for 1660 degrees of freedom

It should be noted that the value of the χ^2 per degree of freedom is unusually small. This is probably because the partial-wave analysis programme does not take into account the correlation terms among the coefficients The coefficients for which the χ^2 per data point is particularly small are those associated with the polarisation, presumably because of the severe mathematical bounds on these values.

The overall features of the data are well described by this solution as can be seen

Table 6
Resonant amplitudes considered for $\bar{K}N \to \pi\Sigma(1385)$, note that our convention is meson first, baryon second in both the initial and the final states

Resonance	Status	Elasticity [a] (x)	Outgoing wave	$t_{\pi\Sigma(1385)}$	Predictions [26] of $t_{\pi\Sigma(1385)}$ [b] from $SU(6)_W \otimes O(3)$ fits	Branching fraction into $\pi\Sigma(1385)$
S01(1825)	Possible	0 37 ± 0 05	D	−0 056 ± 0 028	−0 128	0 008
P03(1900)	Established	0 18 ± 0 02	P	<0 030	+0 05	
			F	+0 126 ± 0 055	−0 100	0 088
D13(1920)	Possible	<0 04	S	−0 066 ± 0 025	−0 177	>0 109
			D		+0 018	
D05(1830)	Established	0 04 ± 0 03	D	−0 141 ± 0 014	0	0 497
			G	<0 030	0	
D15(1775)	Established	0 41 ± 0 03	D	+0 184 ± 0 011	+0 115	0 083
			G	<0 030		
F05(1820)	Established	0 57 ± 0 02	P	+0 167 ± 0 054	+0 215	0 049
			F	−0 065 ±0.029	−0 091	0 007
F05(2100)	Possible	0 07 ± 0 03	P	−0 071 ± 0 025		0 072
			F	<0 03		
F15(1906) Width 135 MeV	Established	0 05 ± 0 03	P	<0 01	−0 035	
			F	−0 039 ± 0 009	+0 021	0 030
F17(2040)	Established	0.24 ± 0 02	F	−0 153 ± 0 026	−0 127	0.098
			H			

[a] From ref [15]
[b] The values listed are with the exception of the D13 amplitudes the predictions of fit 1 of ref [26] in which only the established resonances were used The values for the D13 amplitudes are the predictions of fit 2 of ref [26] The overall sign is arbitrary and we have chosen it to obtain maximum agreement with the measured amplitudes

from figs. 6 and 7. However, the c m. energy region 1770–1810 MeV is comparatively poorly fitted Efforts to improve the fit to the data in this region with one or

Table 7

$K^- p \to \pi\Sigma(1385)$ partial-wave amplitudes, given as real and imaginary parts at 10 MeV centre-of-mass energy intervals for $\Sigma(1385)$ decaying into $\Lambda\pi$

ECM	SD01	PP01	PP03	PF03	DS03	DD03	DD05	DG05	FP05	FF05
1 77	-0 018 -0 036	0 083 -0 177	-0 014 0 050	0 052 -0 016	-0 082 0 023	-0 044 0 003	0 086 -0 037	0 007 0 008	0 065 0 044	-0 021 -0 014
1 78	0 016 0 040	0 087 -0 175	-0 015 0 052	0 058 -0 011	-0 084 0 023	0 046 0 003	-0 092 -0 051	0 008 0 011	0 071 0 064	-0 024 -0 021
1 79	-0 014 -0 044	0 089 -0 172	-0 017 0 053	0 064 -0 006	-0 086 0 024	-0 048 0 004	-0 095 -0 069	0 008 0 014	0 070 0 090	-0 025 -0 031
1 80	-0 010 -0 047	0 092 -0 170	-0 019 0 054	0 069 0 001	-0 088 0 024	-0 051 0 004	-0 091 -0 091	0 008 0 019	0 057 0 121	-0 022 -0 043
1 81	-0 007 -0 050	0 094 -0 167	-0 021 0 056	0 075 0 009	-0 089 0 025	-0 053 0 004	-0 077 -0 112	0 006 0 024	0 027 0 146	-0 012 -0 055
1 82	-0 002 -0 052	0 096 -0 163	-0 023 0 057	0 080 0 017	-0 091 0 025	-0 055 0 004	-0 054 -0 127	0 001 0 028	-0 012 0 155	0 002 -0 061
1 83	0 002 -0 053	0 098 -0 160	-0 025 0 059	0 085 0 028	-0 093 0 026	-0 058 0 004	-0 026 -0 129	-0 004 0 031	-0 048 0 145	0 017 -0 059
1 84	0 007 -0 054	0 099 -0 156	-0 027 0 060	0 089 0 039	-0 095 0 026	-0 060 0 005	-0 002 -0 120	-0 010 0 031	-0 073 0 125	0 027 -0 053
1 85	0 011 -0 053	0 101 -0 152	-0 028 0 063	0 093 0 054	-0 097 0 027	-0 062 0 005	0 013 -0 105	-0 014 0 030	-0 085 0 103	0 034 -0 046
1 86	0 015 0 052	0 102 -0 147	-0 031 0 066	0 095 0 072	-0 098 0 027	-0 064 0 005	0 021 -0 089	-0 017 0 028	-0 091 0 085	0 038 -0 040
1 87	0 019 0 051	0 102 -0 143	-0 034 0 069	0 094 0 094	-0 100 0 028	-0 066 0 005	0 024 -0 074	-0 019 0 026	-0 093 0 070	0 039 -0 034
1 88	0 022 -0 049	0 103 -0 138	-0 038 0 074	0 085 0 121	-0 102 0 028	-0 069 0 005	0 024 -0 062	-0 021 0 024	-0 092 0 058	0 040 -0 030
1 89	0 025 -0 047	0 103 -0 133	-0 045 0 078	0 062 0 148	-0 103 0 029	-0 071 0 005	0 021 -0 052	-0 021 0 023	-0 091 0 048	0 041 -0 026
1 90	0 027 -0 045	0 102 -0 127	-0 055 0 079	0 027 0 163	-0 105 0 029	-0 073 0 006	0 018 -0 044	-0 022 0 022	-0 090 0 040	0 041 -0 023
1 91	0 029 -0 042	0 102 -0 122	-0 064 0 077	-0 010 0 160	-0 106 0 030	-0 075 0 006	0 014 -0 037	-0 023 0 022	-0 088 0 034	0 041 -0 020
1 92	0 031 -0 040	0 101 -0 117	-0 071 0 072	-0 038 0 145	-0 108 0 030	-0 077 0 006	0 011 -0 032	-0 023 0 021	-0 087 0 028	0 041 -0 018
1 93	0 032 -0 038	0 100 -0 111	-0 076 0 068	0 054 0 126	-0 109 0 030	-0 079 0 006	0 007 -0 028	-0 023 0 021	-0 086 0 023	0 041 -0 016
1 94	0 032 -0 035	0 098 -0 105	-0 080 0 063	-0 063 0 109	-0 111 0 031	-0 081 0 006	0 003 -0 024	-0 024 0 021	-0 085 0 018	0 041 -0 015
1 95	0 033 -0 033	0 096 -0 100	-0 082 0 059	-0 068 0 094	-0 112 0 031	-0 083 0 006	-0 000 -0 021	-0 024 0 022	-0 084 0 014	0 041 -0 013
1 96	0 033 -0 031	0 094 -0 094	-0 085 0 056	-0 070 0 082	-0 114 0 032	-0 084 0 006	-0 003 -0 019	-0 024 0 022	-0 084 0 010	0 042 0 011
1 97	0 034 -0 030	0 091 -0 088	-0 087 0 053	-0 071 0 071	-0 115 0 032	-0 086 0 007	-0 007 -0 016	-0 025 0 022	-0 083 0 005	0 042 -0 010
1 98	0 034 -0 028	0 088 -0 082	-0 090 0 051	-0 071 0 061	-0 116 0 032	-0 088 0 007	-0 010 -0 015	-0 025 0 023	-0 083 0 001	0 042 -0 008
1 99	0 034 -0 026	0 085 -0 076	-0 092 0 048	-0 071 0 052	-0 118 0 033	-0 090 0 007	-0 012 -0 013	-0 025 0 023	-0 082 -0 004	0 042 -0 006
2 00	0 033 -0 025	0 082 -0 071	-0 095 0 046	-0 069 0 044	-0 119 0 033	-0 091 0 007	-0 015 -0 012	-0 026 0 024	-0 082 -0 009	0 042 -0 004
2 01	0 033 -0 024	0 078 -0 065	-0 097 0 043	-0 067 0 036	-0 120 0 033	-0 093 0 007	-0 018 -0 010	-0 026 0 024	-0 081 -0 014	0 042 -0 002
2 02	0 033 -0 022	0 074 -0 059	-0 099 0 040	-0 063 0 029	-0 122 0 034	-0 095 0 007	-0 020 -0 009	-0 027 0 025	-0 080 -0 020	0 042 -0 000
2 03	0 033 -0 021	0 069 -0 054	-0 102 0 038	-0 059 0 023	-0 123 0 034	-0 096 0 007	-0 023 -0 008	-0 027 0 026	-0 077 -0 026	0 042 0 002
2 04	0 032 0 020	0 064 -0 048	-0 104 0 035	-0 054 0 018	-0 124 0 034	-0 098 0 007	-0 025 -0 007	-0 027 0 026	-0 075 -0 032	0 041 0 004
2 05	0 032 -0 019	0 059 -0 042	-0 107 0 032	-0 048 0 013	-0 125 0 035	-0 100 0 008	-0 027 -0 006	-0 028 0 027	-0 071 -0 038	0 040 0 006
2 06	0 032 0 018	0 054 -0 037	-0 109 0 029	-0 041 0 010	-0 126 0 035	-0 101 0 008	-0 029 -0 006	-0 028 0 028	-0 066 -0 043	0 039 0 009
2 07	0 031 0 017	0 048 -0 032	-0 112 0 026	-0 034 0 009	-0 128 0 035	-0 103 0 008	-0 031 -0 005	-0 029 0 029	-0 060 -0 048	0 037 0 011
2 08	0 031 -0 016	0 042 -0 027	-0 114 0 023	-0 027 0 008	-0 129 0 036	-0 104 0 008	-0 033 -0 004	-0 029 0 030	-0 053 -0 051	0 035 0 012
2 09	0 031 -0 016	0 036 -0 022	-0 116 0 019	-0 019 0 010	-0 130 0 036	-0 106 0 008	-0 035 -0 004	-0 029 0 031	-0 046 -0 054	0 033 0 013
2 10	0 030 -0 015	0 029 -0 017	-0 118 0 016	-0 012 0 012	-0 131 0 036	-0 107 0 008	-0 037 -0 003	-0 030 0 031	-0 038 -0 055	0 030 0 014
2 11	0 030 -0 014	0 022 -0 012	-0 120 0 012	-0 005 0 017	-0 132 0 037	-0 109 0 008	-0 039 -0 003	-0 030 0 032	-0 031 -0 054	0 028 0 014
2 12	0 029 -0 014	0 015 -0 008	-0 122 0 009	0 001 0 023	-0 133 0 037	-0 110 0 008	-0 040 -0 002	-0 031 0 033	-0 024 -0 053	0 025 0 014
2 13	0 029 -0 013	0 007 -0 004	-0 124 0 005	0 006 0 030	-0 134 0 037	-0 111 0 008	-0 042 -0 002	-0 031 0 034	-0 019 -0 051	0 023 0 014
2 14	0 029 -0 013	-0 000 0 000	-0 126 0 001	0 010 0 038	-0 135 0 038	-0 113 0 009	-0 043 -0 001	-0 031 0 035	-0 014 -0 048	0 021 0 013
2 15	0 028 -0 012	-0 008 0 004	-0 127 -0 003	0 013 0 048	-0 136 0 038	-0 114 0 009	-0 045 -0 001	-0 032 0 036	-0 010 -0 044	0 020 0 012
2 16	0 028 -0 012	-0 016 0 007	-0 129 -0 007	0 014 0 059	-0 137 0 038	-0 115 0 009	-0 047 -0 000	-0 032 0 037	-0 007 -0 041	0 019 0 011
2 17	0 028 -0 011	-0 025 0 011	0 130 -0 012	0 013 0 071	-0 138 0 038	-0 116 0 009	-0 048 -0 000	-0 033 0 038	-0 004 -0 038	0 018 0 010

TABLE 7(B)

ECM	SD11	PP11	PP13	PF13	DS13	DD13	DD15	DG15	FP15	FF15	FF17
1 77	0 083 0 176	-0 050 0 007	-0 187 -0 097	0 008 0 006	-0 033 -0 150	-0 025 0 013	0 032 0 149	-0 007 -0 023	0 008 -0 002	-0 014 -0 004	-0 009 -0 001
1 78	0 072 0 184	-0 052 0 007	-0 188 -0 098	-0 008 0 007	-0 025 0 152	-0 027 0 014	0 006 0 152	-0 004 -0 025	0 008 -0 002	-0 016 -0 004	-0 011 -0 002
1 79	0 059 0 192	-0 053 0 007	-0 189 -0 098	-0 009 0 007	-0 017 -0 153	-0 028 0 015	-0 017 0 148	-0 000 -0 026	0 009 -0 002	-0 018 -0 005	-0 012 -0 002
1 80	0 045 0 198	-0 054 0 007	-0 190 -0 098	-0 010 0 008	-0 008 -0 154	0 029 0 015	-0 037 0 138	0 003 -0 026	0 009 -0 002	-0 020 -0 006	-0 014 -0 002
1 81	0 031 0 202	-0 055 0 008	-0 190 -0 098	-0 010 0 009	-0 000 -0 154	0 031 0 016	-0 051 0 125	0 006 -0 026	0 009 -0 003	-0 022 -0 008	-0 016 -0 003
1 82	0 016 0 205	-0 057 0 008	-0 190 -0 099	-0 011 0 009	0 008 0 153	-0 032 0 017	-0 062 0 112	0 008 -0 025	0 009 -0 003	-0 025 -0 010	-0 018 -0 004
1 83	0 001 0 206	-0 058 0 008	-0 190 -0 098	-0 012 0 010	0 016 -0 152	-0 034 0 017	-0 068 0 098	0 009 -0 023	0 010 -0 003	-0 027 -0 012	-0 020 -0 005
1 84	-0 014 0 205	-0 059 0 008	-0 189 -0 098	-0 013 0 010	0 024 -0 150	-0 035 0 018	-0 072 0 086	0 011 -0 022	0 010 0 004	-0 030 -0 016	-0 023 -0 006
1 85	-0 029 0 203	-0 060 0 008	-0 189 -0 098	-0 013 0 011	0 032 -0 148	-0 036 0 019	-0 074 0 074	0 011 -0 021	0 010 -0 004	-0 032 -0 019	-0 025 -0 007
1 86	-0 043 0 199	-0 061 0 008	-0 188 -0 097	-0 014 0 012	0 040 -0 145	-0 037 0 019	-0 074 0 064	0 012 -0 020	0 011 -0 005	-0 033 -0 024	-0 028 -0 009
1 87	-0 057 0 194	-0 062 0 009	-0 186 -0 097	-0 015 0 012	0 047 -0 142	-0 039 0 020	-0 074 0 055	0 012 0 019	0 011 -0 005	-0 033 -0 029	-0 032 -0 011
1 88	-0 070 0 187	-0 063 0 009	-0 185 -0 096	-0 016 0 013	0 054 -0 137	-0 040 0 021	-0 072 0 047	0 012 -0 018	0 012 -0 006	-0 032 -0 034	-0 035 -0 013
1 89	0 082 0 179	-0 064 0 009	-0 183 -0 095	-0 016 0 014	0 061 -0 133	-0 041 0 021	-0 071 0 040	0 012 -0 017	0 013 -0 006	-0 029 -0 038	-0 039 -0 016
1 90	-0 094 0 169	-0 065 0 009	-0 182 -0 094	-0 017 0 014	0 067 -0 127	-0 042 0 022	-0 069 0 033	0 012 -0 016	0 014 -0 006	-0 025 -0 041	-0 043 -0 020
1 91	-0 104 0 159	-0 066 0 009	-0 180 -0 093	-0 018 0 015	0 073 -0 121	-0 044 0 022	-0 067 0 028	0 012 -0 015	0 015 -0 006	-0 021 -0 042	-0 047 -0 024
1 92	0 112 0 148	-0 067 0 009	-0 177 -0 092	-0 019 0 016	0 079 -0 115	-0 045 0 023	-0 065 0 022	0 011 -0 014	0 016 -0 006	-0 017 -0 042	-0 051 0 029
1 93	-0 120 0 135	-0 068 0 009	-0 175 -0 091	-0 020 0 016	0 084 -0 108	-0 046 0 024	-0 062 0 018	0 011 -0 013	0 017 -0 006	-0 014 -0 041	-0 055 -0 036
1 94	-0 126 0 123	-0 069 0 009	-0 172 -0 089	-0 020 0 017	0 087 -0 100	-0 047 0 024	-0 060 0 013	0 010 -0 012	0 017 -0 006	-0 012 -0 039	-0 059 -0 043
1 95	-0 130 0 110	0 070 0 010	-0 170 -0 088	-0 021 0 017	0 090 -0 092	-0 048 0 025	-0 058 0 010	0 009 -0 011	0 018 -0 006	-0 011 -0 037	-0 062 -0 052
1 96	0 133 0 096	-0 070 0 010	-0 167 -0 087	-0 022 0 018	0 092 -0 084	-0 049 0 025	-0 056 0 006	0 009 -0 011	0 018 -0 005	-0 011 -0 035	-0 064 -0 063
1 97	-0 134 0 083	-0 071 0 010	-0 164 -0 085	-0 023 0 019	0 093 -0 076	-0 050 0 026	-0 053 0 003	0 008 -0 010	0 019 -0 005	-0 011 -0 033	-0 064 -0 075
1 98	-0 134 0 070	-0 072 0 010	-0 161 -0 083	-0 024 0 019	0 093 -0 069	-0 051 0 026	0 051 -0 000	0 007 -0 009	0 019 -0 005	-0 011 -0 031	-0 062 -0 088
1 99	-0 132 0 057	-0 073 0 010	-0 157 -0 082	-0 024 0 020	0 092 -0 061	-0 052 0 027	-0 049 -0 003	0 006 -0 009	0 020 -0 005	-0 012 -0 030	-0 058 -0 102
2 00	-0 129 0 045	-0 074 0 010	-0 154 -0 080	-0 025 0 021	0 091 -0 054	-0 053 0 027	-0 047 -0 006	0 005 -0 008	0 020 -0 005	-0 013 -0 028	-0 050 -0 115
2 01	-0 124 0 033	-0 074 0 010	-0 150 -0 078	-0 026 0 021	0 088 -0 047	-0 054 0 028	-0 045 -0 009	0 004 -0 007	0 020 -0 005	-0 014 -0 027	-0 038 -0 127
2 02	-0 118 0 023	-0 075 0 010	-0 146 -0 076	-0 027 0 022	0 084 -0 041	-0 055 0 028	-0 043 -0 011	0 003 -0 007	0 020 -0 004	-0 016 -0 026	-0 024 0 137
2 03	-0 111 0 013	-0 076 0 011	-0 142 -0 074	-0 027 0 022	0 080 -0 036	-0 056 0 029	-0 041 -0 013	0 002 -0 006	0 021 -0 004	-0 017 -0 025	-0 008 -0 142
2 04	-0 102 0 005	-0 077 0 011	-0 138 -0 072	-0 028 0 023	0 076 -0 031	-0 057 0 029	-0 039 -0 015	0 000 -0 005	0 021 -0 004	-0 018 -0 025	0 008 -0 144
2 05	-0 093 0 003	-0 077 0 011	-0 134 -0 070	-0 029 0 024	0 071 -0 027	-0 058 0 030	-0 037 -0 017	-0 001 -0 005	0 021 -0 004	-0 020 -0 024	0 024 -0 143
2 06	-0 083 -0 009	-0 078 0 011	-0 130 -0 067	-0 030 0 024	0 066 -0 024	-0 059 0 030	-0 036 -0 019	-0 002 -0 004	0 022 -0 004	-0 021 -0 024	0 038 0 138
2 07	-0 073 0 013	-0 079 0 011	-0 125 -0 065	-0 030 0 025	0 061 -0 022	-0 060 0 031	-0 034 -0 021	-0 004 -0 003	0 022 -0 004	-0 023 -0 023	0 049 -0 132
2 08	-0 062 -0 016	-0 079 0 011	-0 121 -0 063	-0 031 0 025	0 055 -0 021	-0 061 0 031	-0 032 -0 023	-0 005 -0 003	0 022 -0 004	-0 024 -0 023	0 059 -0 124
2 09	-0 051 -0 017	-0 080 0 011	-0 116 -0 060	-0 032 0 026	0 050 -0 021	-0 062 0 032	-0 031 -0 024	-0 006 -0 002	0 022 -0 004	-0 026 -0 023	0 066 -0 116
2 10	-0 040 -0 017	-0 081 0 011	-0 111 -0 058	-0 032 0 027	0 045 -0 022	-0 062 0 032	-0 029 -0 026	-0 008 -0 001	0 022 -0 004	-0 027 -0 022	0 071 0 108
2 11	-0 029 -0 014	-0 081 0 011	-0 106 -0 055	-0 033 0 027	0 040 -0 023	-0 063 0 033	-0 027 -0 027	-0 009 -0 001	0 023 -0 004	-0 029 -0 022	0 075 -0 100
2 12	-0 018 0 011	-0 082 0 011	-0 101 -0 053	-0 034 0 028	0 035 -0 026	-0 064 0 033	-0 026 -0 029	-0 011 0 000	0 023 -0 004	-0 030 -0 022	0 078 0 093
2 13	-0 008 -0 006	-0 083 0 011	-0 096 -0 050	-0 034 0 028	0 031 -0 029	-0 065 0 033	-0 024 -0 030	-0 012 0 001	0 023 -0 004	-0 031 -0 022	0 080 -0 086
2 14	0 002 0 001	-0 083 0 012	-0 091 -0 047	-0 035 0 029	0 028 -0 032	-0 066 0 034	-0 023 -0 032	-0 014 0 001	0 023 -0 004	-0 033 -0 022	0 080 -0 080
2 15	0 010 0 010	-0 084 0 012	-0 086 -0 045	-0 035 0 029	0 025 -0 036	-0 066 0 034	-0 022 -0 033	-0 016 0 002	0 024 -0 004	-0 034 -0 022	0 081 -0 074
2 16	0 018 0 019	-0 084 0 012	-0 081 -0 042	-0 036 0 030	0 023 -0 041	-0 067 0 035	-0 020 -0 034	-0 017 0 003	0 024 -0 004	-0 036 -0 022	0 081 0 069
2 17	0 024 0 030	-0 085 0 012	-0 075 -0 039	-0 037 0 030	0 021 -0 047	-0 068 0 035	-0 019 -0 035	-0 019 0 003	0 024 -0 004	-0 037 0 022	0 080 -0 065

Figure 8(a)

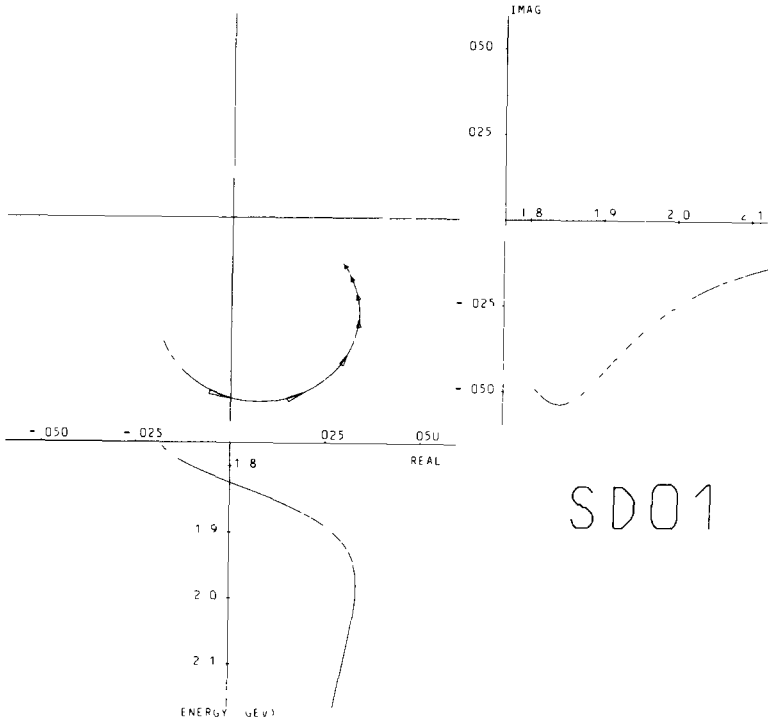

Figure 8(b)

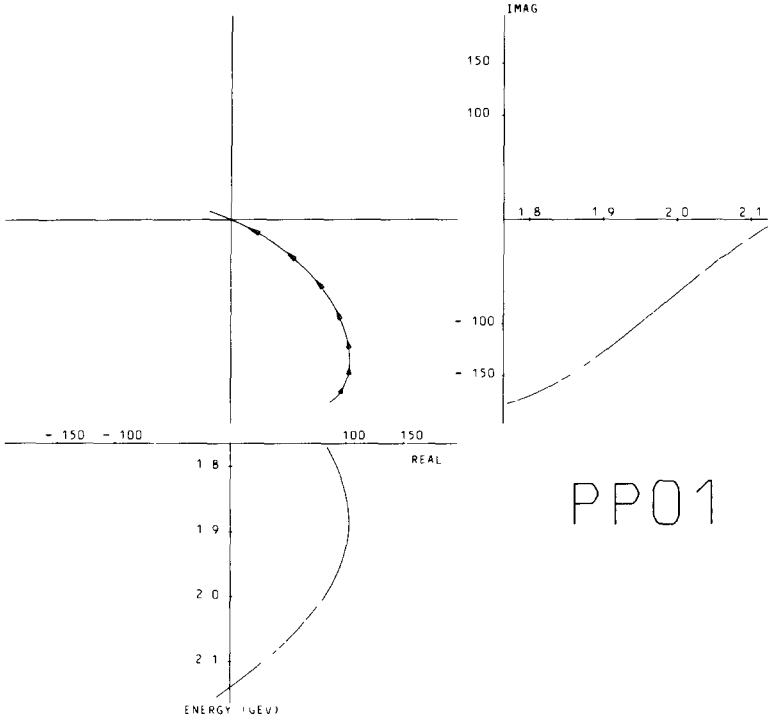

Figure 8(c)

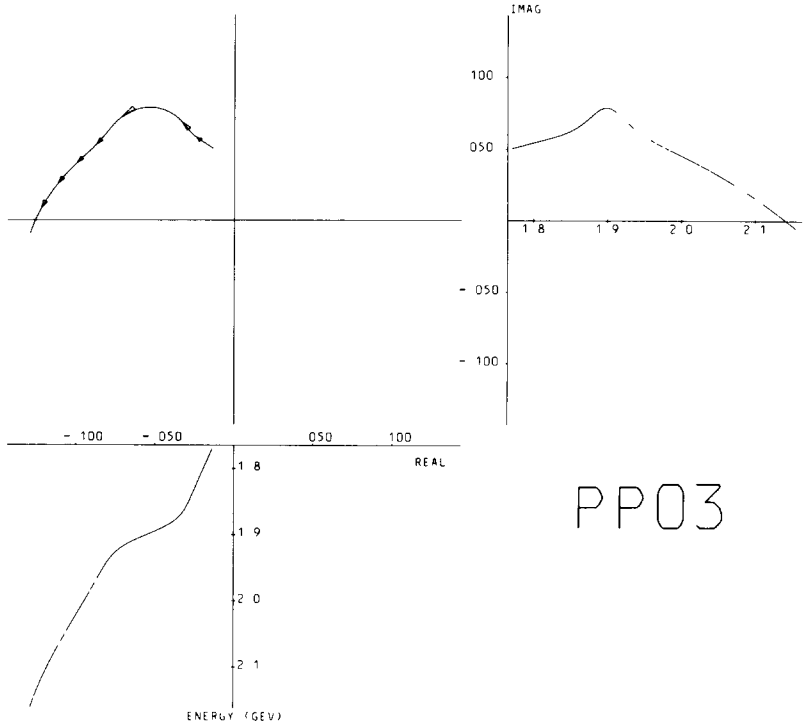

Figure 8(d)

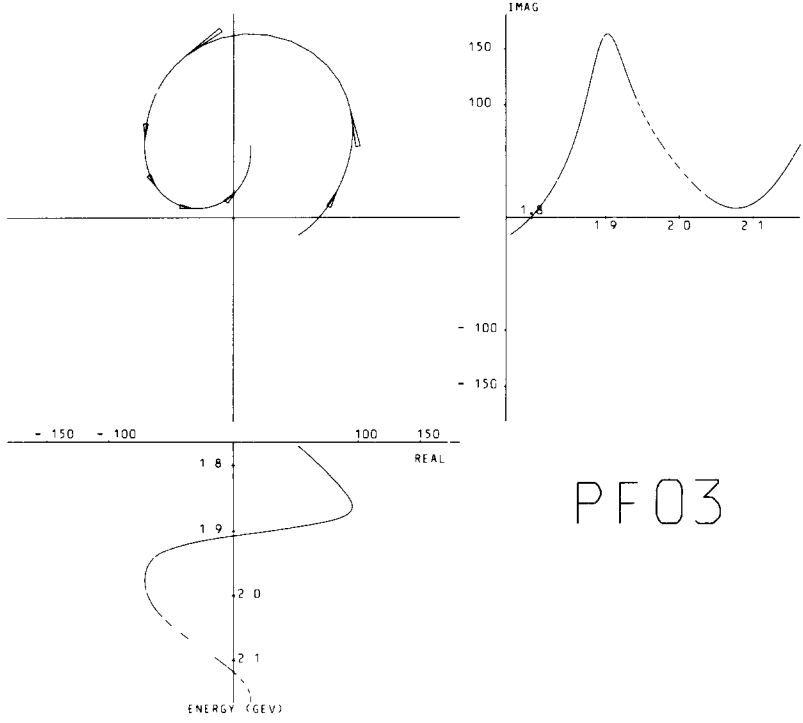

Figure 8(e)

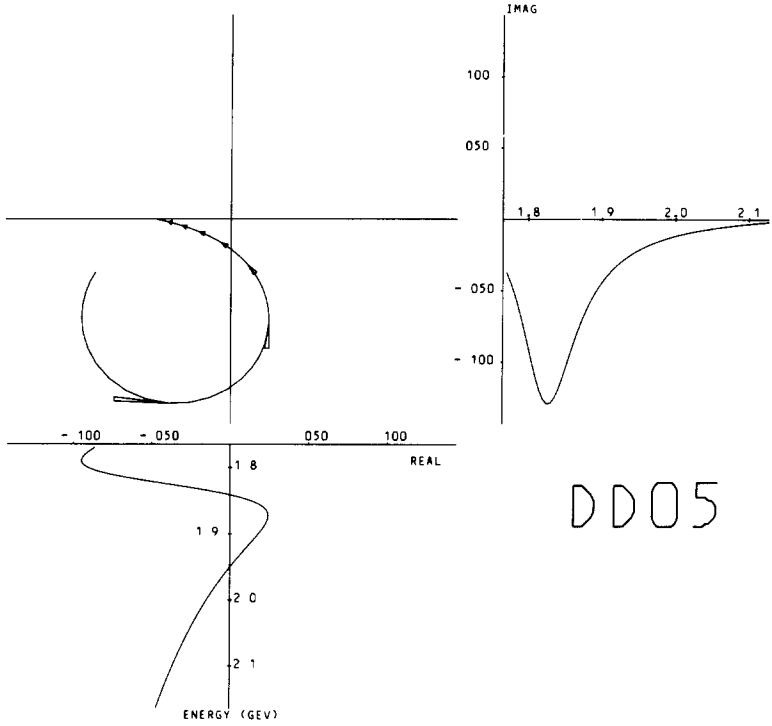

Figure 8(f)

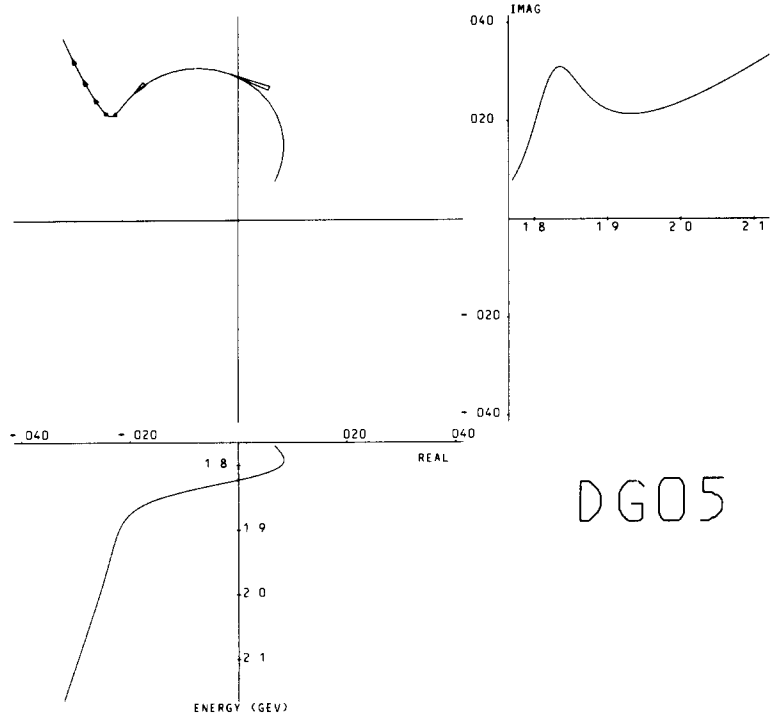

Figure 8(g)

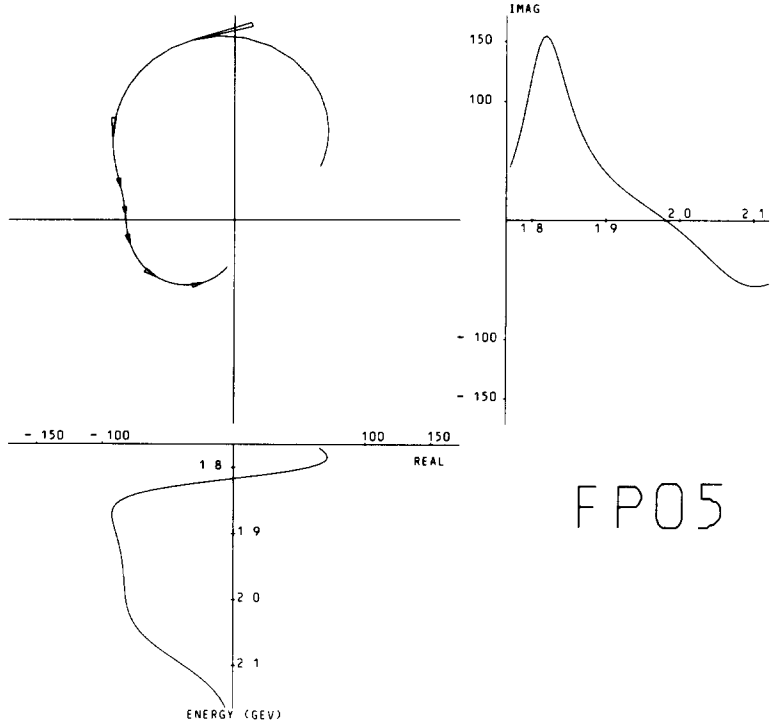

Figure 8(h)

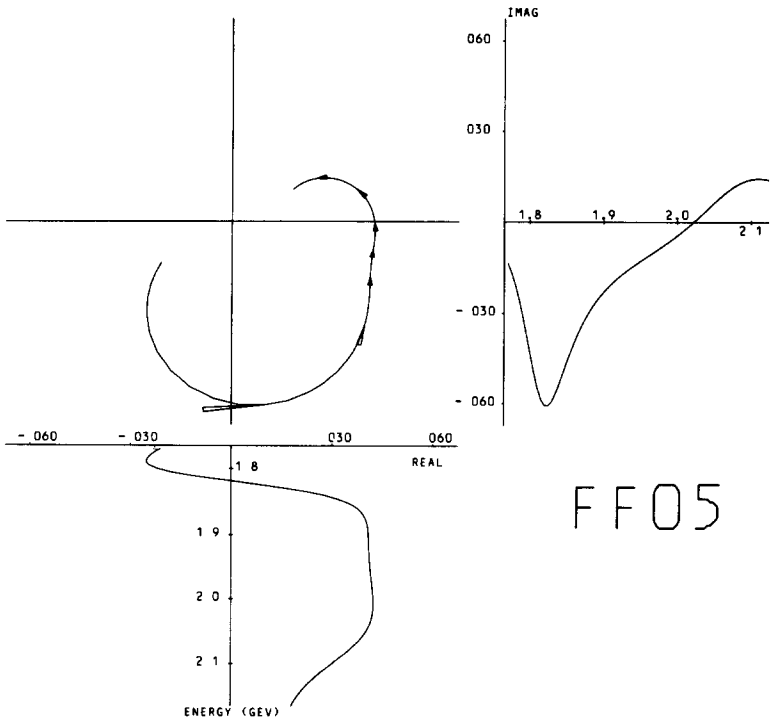

Figure 8(i)

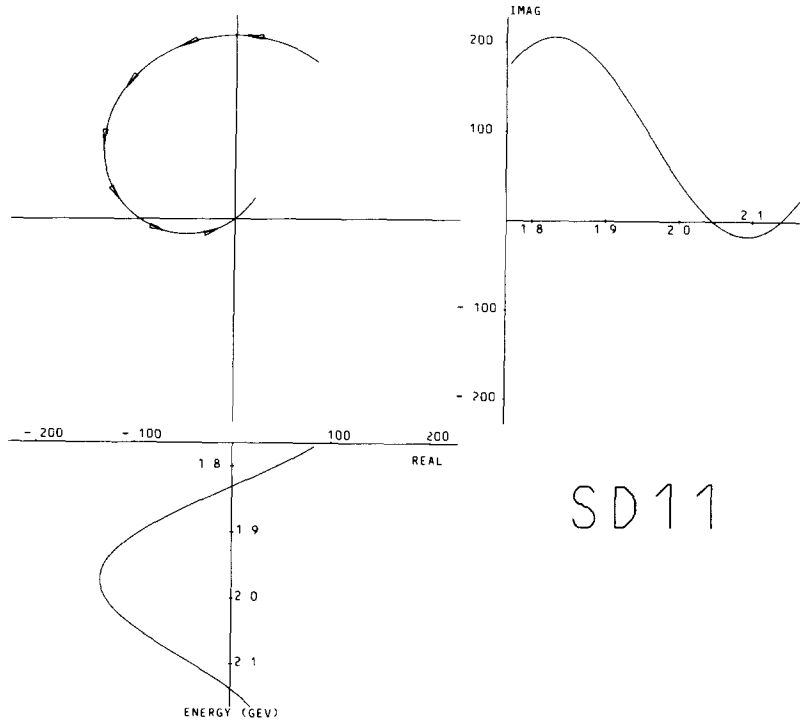

Figure 8(j)

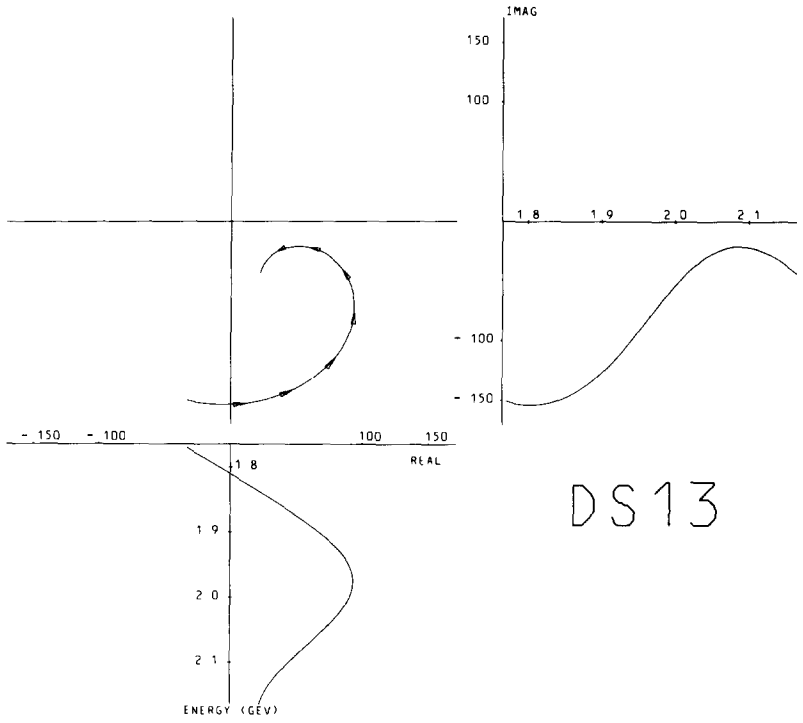

Figure 8(k)

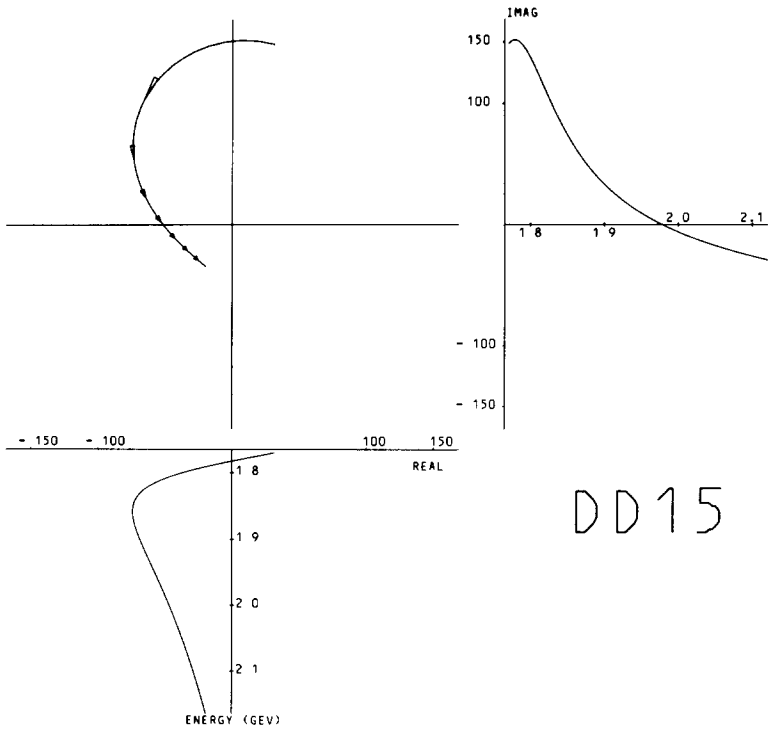

Figure 8(l)

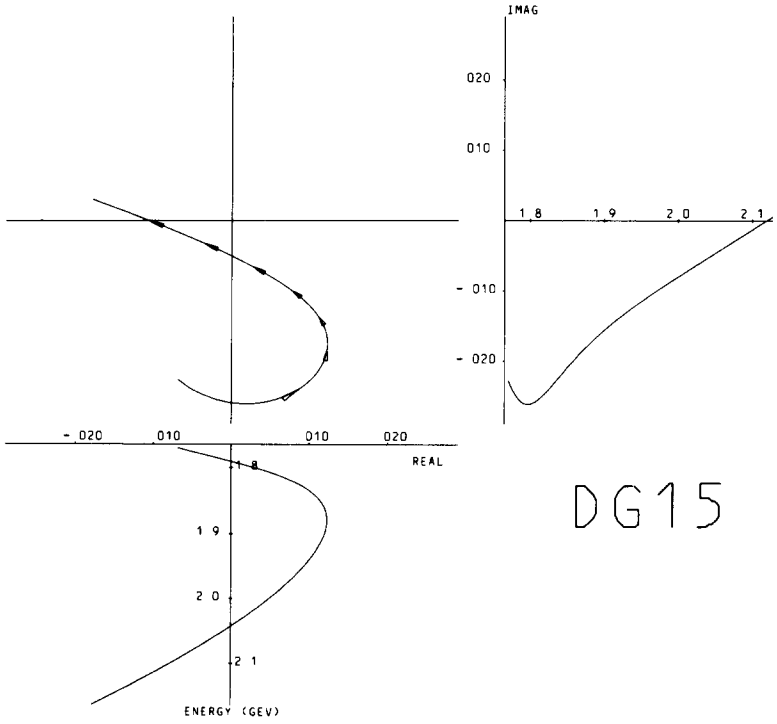

Figure 8(m)

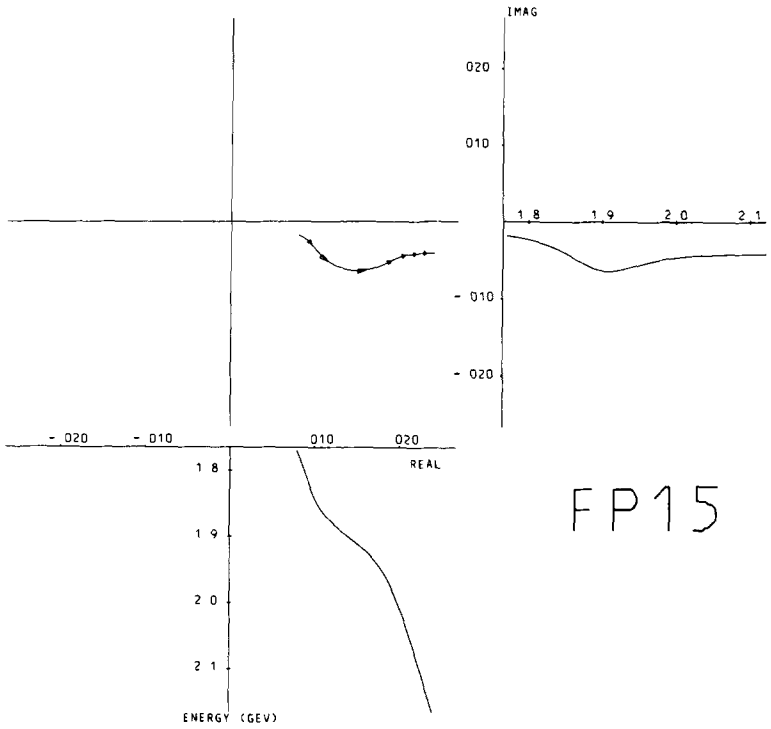

Figure 8(n)

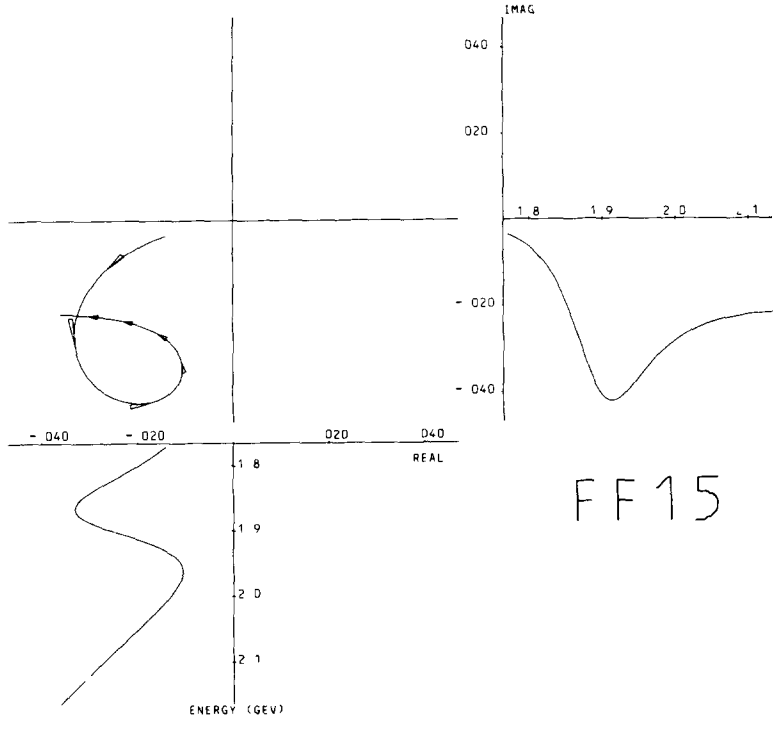

Figure 8(o)

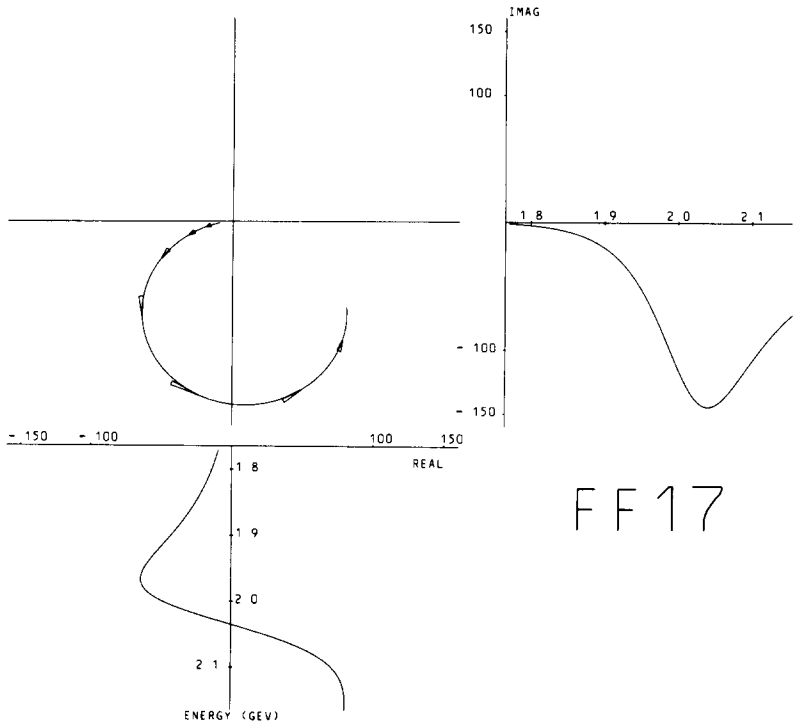

Fig 8 Argand diagrams for the active partial waves. The arrows are 12 5 MeV long, spaced at 50 MeV intervals

more resonances having widths greater than 30 MeV were unsuccessful. It would require higher statistics to allow for finer binning in this energy region to resolve any narrow structures. The resonant amplitudes obtained in the final fit are given in table 6. The partial-wave amplitudes are presented at every 10 MeV c.m. energy interval in table 7, and the Argand diagrams for the active partial waves are shown in fig.8.

5. Comparison with SU(3)

Having assigned resonances into SU(3) multiplets, it is then possible in certain cases to predict the relative signs of resonance amplitudes. The D05(1830) and D15(1755) are both members of the $\frac{5}{2}^-$ octet and using the accepted value for the F- and D-admixture parameter (α) for their coupling to the initial K^-p state the relative sign of their D-wave decay amplitudes to $\pi\Sigma(1385)$ is predicted to be negative We find this to be the case in contrast to the results obtained by Prevost et al. [19].

Table 8
Comparison of the signs of resonant amplitudes with those predicted by SU(3) from $\pi N \to N^*/\Delta \to \pi\Delta$, note that the overall sign is arbitrary

SU(3) multiplet	Resonant amplitude	Observed sign	Predicted sign
$\frac{5}{2}^-$ octet	DD05(1830)	(−)	(−)
	DD15(1775)	+	+
$\frac{5}{2}^+$ octet	FP05(1820)	+	+
	FF05(1820)	−	−
	FF15(1906)	−	−
$\frac{7}{2}^+$ decuplet	FF17(2040)	−	−

The $\pi\Sigma(1385)$ amplitudes can also be related by SU(3) to the $\pi\Delta$ decay of non-strange N^* and Δ resonances, the amplitude signs of many of which have been determined [20]. The signs of amplitudes obtained in the present analysis for members of the $\frac{5}{2}^-$ octet, $\frac{5}{2}^+$ octet and $\frac{7}{2}^+$ decuplet are compared with those derived from $\pi\Delta$ amplitudes in table 8. The five relative signs which may be determined are all as expected. For the F15 amplitude the sign is very sensitive to the value of the admixture parameter α and was obtained using the most recent value reported by Samios et al. [21] and this value is therefore supported. (The analysis of Cashmore et al. [20] uses an earlier value of α and predicts the wrong F15 sign.) It should be noted that the convention used by Cashmore et al [20] (baryon first, meson second in both initial and final states) is related to the convention used in this analysis by an overall sign change, which is not measurable.

6. Classification of Y*'s in $SU(6)_W$

The reaction channel $K^-p \to \pi\Sigma(1385)$ discussed in this paper is an example of SU(3) inelastic scattering, i.e., the initial and final state baryons come from different SU(3) multiplets. Moreover, the initial and final orbital angular momenta may be different. Resonant amplitudes coupled to this channel can therefore in principle put strong constraints on symmetries higher than SU(3), such as $SU(6)_W \otimes O(3)$, which seek to embrace the spins of resonances.

Using an approach based on the Melosh transformation [23], Cashmore, Hey and Litchfield [24–26] have fitted rates of decays of baryons in the $(70, 1^-)$ and $(56, 2^+)$ multiplets into the ground state $(56, 0^+)$ by pseudoscalar meson emission These fits predict couplings in the $\bar{K}N \to \pi\Sigma(1385)$ channel and comparison with the present results (table 6) permits the following observations to be made

(a) Four resonances assigned to the $(70, 1^-)$ namely S01(1825), D13(1920),

D15(1775) and D05(1830) are found to have significant $\pi\Sigma(1385)$ couplings. The measured signs and rough magnitudes of the first three agree with the predictions. However the D05(1830) as an unmixed member of the quark-spin $\frac{3}{2}$ SU(3) octet is predicted to decouple from $\bar{K}N$, yet, as in the 2-body $\Sigma\pi$ channel [15] it is found to have a large resonant amplitude.

(b) There is no evidence for the predicted large amplitudes for the D03(1815) and S11(1930) members of the $(70, 1^-)$

(c) F05(1820), F15(1906) and F17(2040) states assigned to the $(56, 2^+)$ are observed to have significant $\pi\Sigma(1385)$ couplings The F05 and F17 signs are as predicted, and in particular the sign of the P-wave decay amplitude of the F05 confirms the "$SU(6)_W$ like" P/F sign ratio reported in the $\Delta\pi$ analysis [28].

(d) In agreement with prediction, the F15(1906) amplitudes are found to be small in magnitude In view of this the apparent sign disagreement of the F-wave decay amplitude is probably not significant.

(e) A major disagreement occurs in the sign of the large amplitude for the F-wave decay of the P03(1900) when assigned to the $(56, 2^+)$, suggesting that such an assignment is incorrect. It could be a candidate for the $(70, 2^+)$ multiplet predicted by Horgan and Dalitz [22] to be mass degenerate with the $(56, 2^+)$ multiplet. The observation of the F05(2100) in the present analysis and in the $\Sigma\pi$ channel [27,15] provides supporting evidence for that multiplet.

6. Conclusions

New data are presented on the reaction $K^- p \to \Lambda^0 \pi^+ \pi^-$ at eleven energies between 1775 and 1957 MeV in the c.m. These high-statistics data allow the best measurement to date of the masses and widths of the $\Sigma(1385)$ resonance.

The real parts of the density matrix elements for the reactions $K^- p \to \pi^\pm \Sigma^\mp(1385)$ have been extracted in terms of Legendre polynomial expansion coefficients using an incoherent quasi two-body model. The information available from the Λ decay has also been exploited to obtain the polarisation coefficients corresponding to the imaginary parts of the density matrices.

Using these coefficients together with those from the CRSS experiment, an energy dependent partial-wave analysis has been carried out and the couplings of resonances to the $\bar{K}N \to \pi\Sigma(1385)$ channel have been determined. The well established resonances D15(1775), D05(1830), F05(1820), P03(1900) and F17(2040) were found to have significant couplings to this channel. An interesting feature of the solution is that, with the exception of the P03(1900), the partial wave with the lower outgoing orbital angular momentum dominates Of the less well established resonances only the S01(1825), F05(2100) and the D13(1920) are required. It should be noted that as in the $\bar{K}N \to$ two-body channels and the $K^- p \to \pi\Lambda(1520)$ channel [29], there is no evidence for any P13 resonances.

Using SU(3) symmetry, the relative signs of the resonance couplings are found to

be in complete agreement with those predicted from measurements of the $\pi N \to \pi\Delta$ reaction. The results have also been compared with predictions of $SU(6)_W \otimes O(3)$ model fits.

References

[1] A de Bellefon, A. Berthon, L K Rangan, J. Vrana, T C Bacon, A. Brandstetter, I Butterworth, S M Deen, C M. Fisher, P J Litchfield, R J Miller, J R Smith, G Burgun, J Meyer, E Pauli, G Poulard, B Tallini, W Wojcik, J Zatz and R Strub, Nuovo Cim 7A (1972) 567

[2] RL-IC Collaboration, B Conforto, G P. Gopal, G E Kalmus, P J Litchfield, R T Ross, A J. Van Horn, T C Bacon, I Butterworth, E F Clayton and R M Waters, Nucl Phys B105 (1976) 189

[3] RL-IC Collaboration, E.F. Clayton, T C Bacon, I. Butterworth, R M Waters, B Conforto, G P Gopal, G.E. Kalmus, R T Ross and A J. Van Horn, Nucl Phys B95 (1975) 130

[4] M. Jones, R Levi-Setti, D Merrill and R D. Tripp, Nucl Phys B90 (1975) 349

[5] J Griselin, A Givernaud, R Barloutaud, J Prevost, F Grandini, C Kiesling, D E Plane, W. Wittek, P. Baillon, C. Bricman, M Ferro-Luzzi, J O. Petersen, E Burkhardt, H. Oberlack, A Putzer and H. Schleich, Nucl. Phys. B93 (1975) 189

[6] R Armenteros, M Ferro-Luzzi, D.W G.S Leith, R Levi-Setti, A Minten, R D Tripp, H Filthuth, V Hepp, E Kluge, H Schneider, R Barloutaud, P Granet, J Meyer and J P. Porte, Nucl Phys B8 (1968) 233

[7] J.D Jackson, Nuovo Cim 34 (1964) 1

[8] S O. Holmgren, M. Aguilar-Benitez, F Barreiro, R J. Hemingway, M J Losty, R P. Worden, J. Zatz, J.C. Kluyver, G.G.G. Massaro, E.W. Kittel and R.T. Van de Walle, Nucl. Phys. B119 (1977) 261.

[9] S.R. Borenstein, G R Kalbfleisch, R.C Strand, V. Vanderburg and J W Chapman, Phys Rev. D9 (1974) 3006.

[10] Particle Data Group, Rev Mod. Phys 48 (1976) 1

[11] B. Franek, The extraction of quasi-two body processes from 3-body final states, programme EXTRA, Rutherford Laboratory Report RL-77-069/A

[12] S.M Deen, Generalised partial-wave analysis, Rutherford Laboratory Report RPP/H/68

[13] P J Litchfield, private communication

[14] A Berthon, G. Tristram, J Vrana, T C Bacon, A Brandstetter, I Butterworth, G P Gopal, P S Jones, P J Litchfield, M Mandelkern, J Meyer, G Poulard, B Tallini, W Wojcik, J Zatz and R Strub, Nuovo Cim 21A (1974) 146

[15] RL-IC Collaboration, G P Gopal, R T Ross, A J Van Horn, A C McPherson, E F Clayton, T.C Bacon and I Butterworth, Nucl Phys B119 (1977) 362.

[16] J M Blatt and V F Weisskopf, Theoretical nuclear physics, (Wiley, New York, 1952) p. 361

[17] B Franek, Coefficients for partial-wave analysis of two-body reactions with general spins, Rutherford Laboratory Bubble Chamber Research Group Physics Note 110, Rutherford Laboratory Report, to be published

[18] R Stern, Ph D thesis, University of London, unpublished

[19] J Prevost, R. Barloutaud, J Griselin, F Pierre, C Bricman, J O Peterson, J Meyer, H Filthuth and E Kluge, Nucl Phys. B69 (1974) 246

[20] R.J. Cashmore, D W G S. Leith, R S Longacre and A H Rosenfeld, Nucl. Phys B92 (1975) 37

[21] N P Samios, M Goldberg and B T Meadows, Rev Mod Phys. 46 (1974) 49

[22] R Horgan and R H Dalitz, Nucl Phys B66 (1973) 135,
R Horgan, Nucl Phys B71 (1974) 514.

[23] H.J Melosh, Phys Rev. D9 (1974) 1095
[24] A J G Hey, P.J Litchfield and R J Cashmore, Nucl. Phys B95 (1975) 516
[25] R J Cashmore, A J.G Hey and P J Litchfield, Nucl Phys. B98 (1975) 237
[26] P J. Litchfield, R.J Cashmore and A J G. Hey, Rutherford Laboratory Report RL-76-111
[27] A de Bellefon, A Berthon, P Billoir, J M Brunet, G Tristram, J Vrana, B Baccari, G Poulard, D Revel and B Tallini, Nuovo Cim 37A (1977) 175
[28] Review talk by K W J Barnham at the Baryon Resonances conf , Oxford, 1976 and references therein
[29] W. Cameron, B Franek, G.P Gopal, G E Kalmus, A C McPherson, R T Ross, D.H Saxon, T C Bacon, I Butterworth, R W M Hughes, P Newham and R A Stern, Nucl Phys B131 (1977) 399